

AD \_\_\_\_\_

Award Number: DAMD17-00-1-0366

TITLE: Miniaturized DNA Biosensor for Decentralized Breast-Cancer Screening

PRINCIPAL INVESTIGATOR: Joseph Wang, Ph.D.

CONTRACTING ORGANIZATION: New Mexico State University  
Las Cruces, New Mexico 88003

REPORT DATE: June 2002

TYPE OF REPORT: Annual

PREPARED FOR: U.S. Army Medical Research and Materiel Command  
Fort Detrick, Maryland 21702-5012

DISTRIBUTION STATEMENT: Approved for Public Release;  
Distribution Unlimited

The views, opinions and/or findings contained in this report are those of the author(s) and should not be construed as an official Department of the Army position, policy or decision unless so designated by other documentation.

20021024 004

# REPORT DOCUMENTATION PAGE

*Form Approved  
OMB No. 074-0188*

Public reporting burden for this collection of information is estimated to average 1 hour per response, including the time for reviewing instructions, searching existing data sources, gathering and maintaining the data needed, and completing and reviewing this collection of information. Send comments regarding this burden estimate or any other aspect of this collection of information, including suggestions for reducing this burden to Washington Headquarters Services, Directorate for Information Operations and Reports, 1215 Jefferson Davis Highway, Suite 1204, Arlington, VA 22202-4302, and to the Office of Management and Budget, Paperwork Reduction Project (0704-0188), Washington, DC 20503

1. AGENCY USE ONLY (Leave blank)	2. REPORT DATE June 2002	3. REPORT TYPE AND DATES COVERED Annual (1 Jun 01 - 31 May 02)	
4. TITLE AND SUBTITLE Miniaturized DNA Biosensor for Decentralized Breast-Cancer Screening		5. FUNDING NUMBERS DAMD17-00-1-0366	
6. AUTHOR(S) Joseph Wang, Ph.D.			
7. PERFORMING ORGANIZATION NAME(S) AND ADDRESS(ES)  New Mexico State University Las Cruces, New Mexico 88003  E-Mail: joewang@nmsu.edu		8. PERFORMING ORGANIZATION REPORT NUMBER	
9. SPONSORING / MONITORING AGENCY NAME(S) AND ADDRESS(ES)  U.S. Army Medical Research and Materiel Command Fort Detrick, Maryland 21702-5012		10. SPONSORING / MONITORING AGENCY REPORT NUMBER	
11. SUPPLEMENTARY NOTES			
12a. DISTRIBUTION / AVAILABILITY STATEMENT  Approved for Public Release; Distribution Unlimited		12b. DISTRIBUTION CODE	
13. ABSTRACT (Maximum 200 Words)  The use of DNA testing as an important component of breast cancer diagnosis has been increasing rapidly over the past decade. The goal of this project is to develop and characterize an electrochemical biosensing microsystem for the rapid point-of-care genetic screening of breast-cancer. During the second year of this project we introduced innovative electrochemical routes for improving the reliability of devices for genetic screening of breast-cancer. In particular, we have successfully combined the unique amplification features of DNA accumulation or metal nanoparticle networks, with an effective magnetic isolation of the duplex, and a powerful label-free electrical detection for achieving the task of sensitive and selective breast-cancer diagnostics. Additional developmental work, particularly further improvements in the sensitivity and selectivity (through the use of dendritic and PNA probes) along with transforming to a miniaturized flow system, is in progress towards the realization of wide-scale decentralized screening for breast cancer.			
14. SUBJECT TERMS breast cancer, decentralized testing, electrochemical detection		15. NUMBER OF PAGES 45	
		16. PRICE CODE	
17. SECURITY CLASSIFICATION OF REPORT Unclassified	18. SECURITY CLASSIFICATION OF THIS PAGE Unclassified	19. SECURITY CLASSIFICATION OF ABSTRACT Unclassified	20. LIMITATION OF ABSTRACT Unlimited

## **Table of Contents**

COVER.....	1
SF 298.....	2
<b>Introduction.....</b>	<b>4</b>
BODY.....	4
<b>Key Research Accomplishments.....</b>	<b>8</b>
<b>Reportable Outcomes.....</b>	<b>9</b>
<b>Conclusions.....</b>	<b>9</b>
<b>References.....</b>	<b>10</b>
<b>Appendices.....</b>	<b>11</b>

## **Introduction**

Wide-scale genetic testing requires the development of easy-to-use, fast, inexpensive, miniaturized analytical devices. Traditional methods for detecting DNA hybridization are too slow and labor intensive. Biosensors offer a promising alternative for faster, simpler, and cheaper nucleic-acid assays. DNA hybridization biosensors commonly rely on the immobilization of a single-stranded (ss) oligonucleotide probe onto a transducer surface to recognize - by hybridization - its complimentary target sequence.

Electrochemical devices have received considerable attention in the development of sequence-specific DNA hybridization biosensors. Such devices rely on the conversion of the DNA base-pair recognition event into a useful electrical signal. The high sensitivity of such devices, coupled to their compatibility with modern microfabrication technologies, portability, minimal power requirements, low cost (disposability), and independence of optical pathway or sample turbidity, make them excellent candidates for decentralized DNA testing. Direct electrical reading of DNA hybridization thus offers great promise for developing simple, rapid, and easy-to-use, cost-effective DNA sensing devices (in a manner analogous to miniaturized blood-glucose meters). Recent efforts have led to a host of new avenues for electrochemical detection of DNA hybridization (1,2).

The ultimate goal of this research is to develop and characterize a miniaturized biosensing flow system for decentralized genetic screening of breast-cancer. The realization of instant point-of-care DNA testing requires proper attention to major challenges of signal amplification, non-specific binding, mismatch discrimination, as well as the integration of the sample preparation with the actual DNA detection on a single microchip flow platform. Such challenges are being met by coupling innovative biosensor strategies with "Lab-on-Chip" technologies. Such user-friendly operation, on a chip platform, would allow testing for breast cancer to be performed more rapidly, inexpensively, and reliably in a decentralized setting, and will thus accelerate the realization of wide-scale breast-cancer screening.

## **Body: Progress Report**

This report summarizes our activity over the second year of the project (i.e., the 7/01-6/02 period). In accordance to our original objectives our studies have focused on various fundamental and practical aspects of electrical detection of DNA segments specific to the breast-cancer gene BRCA1. As described in this section, we have made a substantial progress, and introduced innovative electrochemical routes for improving the reliability of devices for genetic screening of breast-cancer (based on new label-free and particle-based amplification schemes). This 11-mos activity has already resulted in 5 research papers (published or in press in major journals; see attached list for refs. 3-8), and several invited presentations in major meetings. (Several more publications are expected in the late part of 2002.) Such findings pave the way to major improvements in the biosensing of DNA and offer innovative routes for simple, rapid, and user-friendly devices for breast-cancer screening.

Increased attention has been given recently to label-free electrochemical detection schemes, in which the hybridization event triggers a change in an electrical signal. Label-free procedures greatly simplify the sensing protocol (as they eliminate the need for the indicator

addition/association/detection steps) and offer an instantaneous detection of the duplex formation. For example, this year we introduced a new label-free gene-sensing scheme based on the intrinsic electroactivity of DNA (3; see Appendix). Changes in the guanine oxidation process accrued from the hybridization event have thus been exploited for detecting DNA sequences related to the BRCA1 breast cancer gene. The advantages of such direct label-free hybridization measurements have been combined with the magnetic ‘removal’ of unwanted constituents that commonly hamper such assays (Figure 1). The efficient magnetic separation has thus been shown extremely useful for discriminating against unwanted constituents, including a large excess of co-existing mismatched and non-complementary oligomers, chromosomal DNA, RNA and proteins. A renewable (pencil) graphite electrode was employed for transducing the DNA hybridization event. Further signal amplification of such label-free detection was accomplished via the dramatically enhanced accumulation of purine nucleobases in the presence of copper ions (4; see Appendix). The resulting new protocol involved hybridization of the target to inosine-substituted oligonucleotide probes (captured on magnetic beads), acidic dipurinization of the hybrid DNA, and adsorptive chronopotentiometric stripping measurements of the free nucleobases in the presence of copper ions. Both amplified adenine and guanine peaks have thus been used for detecting the DNA hybridization (Figure 2). Factors influencing the signal enhancement were assessed and optimized. A detection limit of 40 fmol of the E908X-WT breast-cancer target was obtained in connection to 10 min hybridization and 5 min adsorptive-accumulation times. Further improvements (towards the detection of point mutations) are expected by coupling the copper-enhanced label-free assay with the use of PNA probes. The coupling of magnetic hybridization surfaces with label-free electrical detection eliminates the needs for external indicators and advanced surface modification or regeneration schemes, and hence results in a greatly simplified protocol. These label-free DNA assays are currently being adapted to automated microfluidic devices towards the realization of decentralized genetic testing.

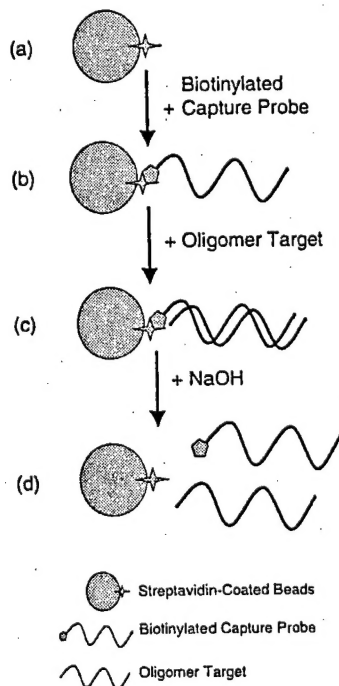
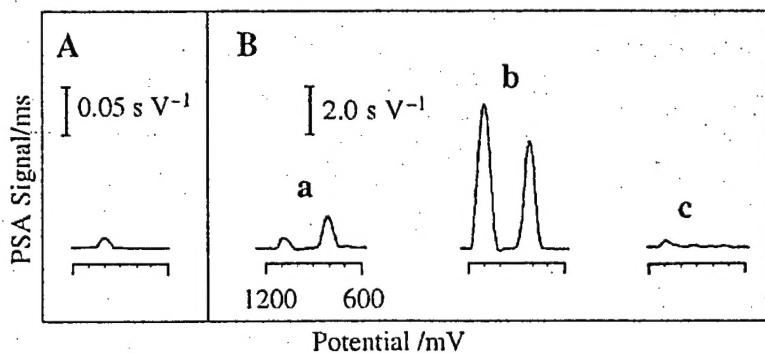


Figure 1. Schematic representation of the analytical protocol: (a) introduction of the streptavidin-coated beads; (b) magnetic capture of the biotinylated probe; (c) hybridization event; (d) release the hybrid DNA from the beads using 0.05 M NaOH solution. (From ref. 3.)



**Figure 2.** Chronopotentiometric stripping hybridization signals to  $2 \text{ mg l}^{-1}$  undigested E908X-WT target (A),  $2 \text{ mg l}^{-1}$  digested E908X-WT target (B(a)),  $2 \text{ mg l}^{-1}$  digested E908X-WT target in presence of  $2 \text{ mg l}^{-1}$  Cu(II) (B(b)),  $200 \text{ mg l}^{-1}$  digested non-complementary (NC) oligomer in presence of  $2 \text{ mg l}^{-1}$  Cu(II), (B(c)). Amount of beads,  $100\mu\text{g}$ ; probe concentration,  $200 \text{ mg l}^{-1}$ ; hybridization time, 10 min; accumulation potential,  $+0.5 \text{ V}$  (A), and  $-0.05 \text{ V}$  (B); accumulation time, 2 min; stripping current,  $+5 \mu\text{A}$  (A), and  $+2 \mu\text{A}$  (B). (From ref. 4.)

Earlier in this Army-sponsored project we developed new nanoparticle-based protocols combining the versatility of microspheres with catalytic enlargement of the metal-particle tags, and the effective ‘built-in’ amplification of electrochemical stripping analysis. During the second year of our activity we introduced a novel nanoparticle-based protocol for detecting DNA hybridization based on a magnetically-induced solid-state electrochemical stripping detection of metal tags (5; see Appendix). Such magnetic triggering of the electrical DNA detection was realized through a ‘magnetic’ collection of the magnetic-bead/DNA-hybrid/metal-tracer assembly onto a thick-film electrode transducer. The new bioassay involves the hybridization of the target breast-cancer oligonucleotide to probe-coated magnetic beads, followed by binding of the streptavidin-coated gold nanoparticles to the captured target, catalytic silver precipitation on the gold-particle tags, a magnetic ‘collection’ of the DNA-linked particle assembly and a solid-state stripping detection (Figure 3, A-E). Such magnetic triggering of the DNA detection is attributed to the facts that the DNA hybrid ‘bridges’ the metal nanoparticles to the magnetic beads (with multiple duplex links per particle) and that most of the three-dimensional DNA-linked aggregate is covered with silver. The new protocol eliminates the acid-dissolution and metal-deposition steps (common to our earlier nanoparticle assays) and hence greatly shortens and simplifies particle-based electrical bioassays. The resulting magnetogenoelectronic method couples high sensitivity with effective discrimination against excess of closely-related nucleotide sequences. Such attractive performance of the

new electrochemical metallogenomagnetic assay is illustrated in Figure 4 for the detection of DNA segments related to the breast-cancer BRCA1 gene in the presence of excess of mismatched and noncomplementary strands. We are currently examining the transformation of particle-based protocols into such microfabricated flow systems (in connection to probe-bearing magnetic beads within the microchannels of such devices). We are also examining multi-amplification assays based on the use of dendritic highly-branched ('tree-like') structures, bearing multiple metal nanoparticle tags.

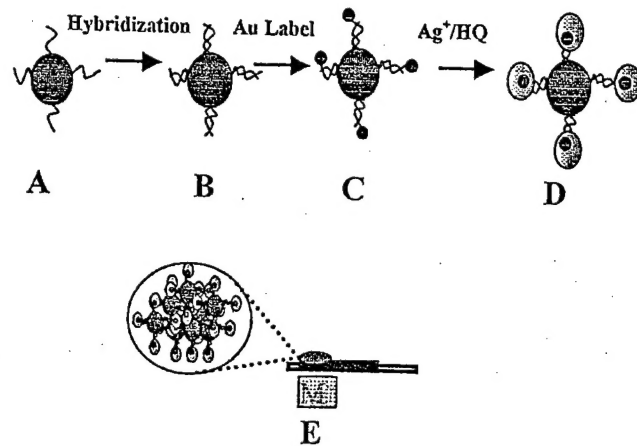


**Figure 3.** Schematic of the magnetically-induced solid-state electrochemical detection of DNA hybridization. (A) Introduction of the probe-coated magnetic beads; (B) the hybridization event (with the biotinylated target); (C) capture of the streptavidin-gold particles; (D) catalytic silver deposition on the gold nanoparticle tags; (E) positioning of an external magnet (M) under the electrode to attract the particle-DNA assembly and solid-state chronopotentiometric detection. (From ref. 5.)

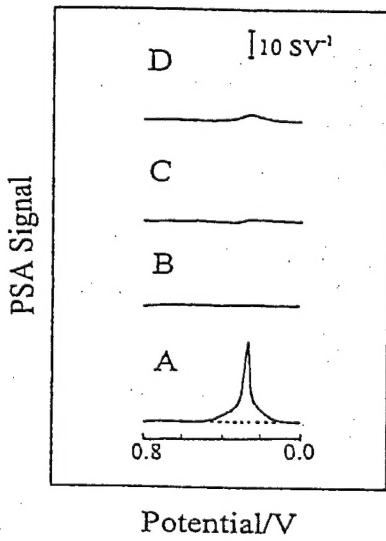


**Figure 4.** Chronopotentiometric hybridization signals for (A) the  $200 \text{ ng mL}^{-1}$  BRCA1 DNA target (with and without an external magnet; solid and dotted lines, respectively), (B)  $20 \mu\text{g mL}^{-1}$  non-complementary strand, (C)  $600 \text{ ng mL}^{-1}$  3-base mismatched oligomer, and (D)  $200 \text{ ng mL}^{-1}$  one-point mutated oligonucleotide. Hybridization time, 20 min; silver enhancement time, 10 min (From ref. 5.)

We also demonstrated a new reversible and cyclic magnetic-field stimulated DNA oxidation (6; see Appendix). Positioning an external magnet below the electrode was shown

to attract the DNA-functionalized magnetic particles to the surface, and stimulate the oxidation of the guanine nucleobases (Figure 5). Using a dual carbon-paste electrode assembly we thus demonstrates a spatially-controlled DNA oxidation, with an ‘On/Off’ switching of the electron-transfer reaction upon relocating the external magnetic field. The site-specific activation of the DNA oxidation holds promise for new DNA arrays and other genoelectronic applications. The influence of relevant experimental variables was examined and optimized. We also described in the same study a new magnetic carbon-paste transducer, combining the solution-phase magnetic separation with an instantaneous magnetic collection of the bead-captured hybrid.

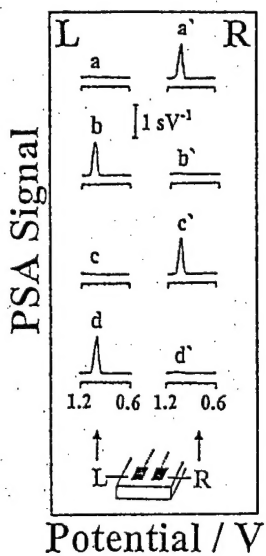


Figure 5. Reversible and cyclic magnetic-field stimulated DNA oxidation: chronopotentiometric guanine signals using the dual-carbon paste electrode assembly. a, b, c, and d are potentiograms obtained at the ‘left’ (L) electrode, while a’, b’, c’, and d’ are potentiograms obtained at the ‘right’ (R) electrode. a, b’, c, and d’ are potentiograms obtained in absence of the magnet, while a’, b, c’, and d are potentiograms recorded in the presence of the magnet. (From Ref. 6.)

## Key Research Accomplishments

During the second year of this project we introduced innovative electrochemical routes for improving the reliability of devices for genetic screening of breast-cancer. In particular, we have successfully combined the unique amplification features of new metal nanoparticles assemblies or of copper-enhanced guanine accumulation, with a powerful magnetically-stimulated electrical detection as well as a label-free transduction, an efficient magnetic removal of non-complementary DNA, use of microliter sample volumes and of disposable transducers for achieving the task of selective, sensitive, and simplified breast-cancer screening (3-6). Such developments address the challenges of mismatch discrimination, signal amplification, non-specific adsorbates, and should facilitate the realization of instant point-of-care breast-cancer testing. The successful realization of such testing will rely (during the 3<sup>rd</sup> year effort) on the transformation of the new label-free and particle-based protocols into miniaturized flow systems (discussed in the Conclusions Section).

## **Reportable Outcomes**

### Papers submitted, accepted or published:

- a. "Magnetic-beads based Label-Free Electrochemical Detection of DNA Hybridization", J. Wang, A. Nasser, A. Erdem, M. Salazare, *Analyst*, 126(2001)2020.
- b. "Amplified Label-Free Detection of DNA Hybridization", J. Wang, and A. Kawde, *Analyst*, 127(2002)383.
- c. "Genomagnetic Electrochemical Assays of DNA Hybridization", J. Wang, D. Xu, R. Polsky, and E. Arzum, *Talanta*, 56(2002)931.
- d. "Magnetically-Induced Solid-State Electrochemical Detection of DNA Hybridization", J. Wang, D. Xu, and R. Polsky, *J. Am. Chem. Soc.*, 124(2002)4208.
- e. "Magnetic Field Stimulated DNA Oxidation", J. Wang and A. Kawde, *Electrochemistry Communications*, 4(2002)349.
- f. "Metal-Nanoparticle Based Electrochemical Stripping Detection of DNA Hybridization", J. Wang, D. Xu, R. Polsky, and A. Kawde, *Anal. Chem.* 73(2001)5576.
- g. "Silver-Enhanced Colloidal Gold Electrical Detection of DNA Hybridization", J. Wang, R. Polsky, D. Xu, *Langmuir*, 17(2001)5739.
- h. "Electrochemical Nucleic Acid Biosensors", (invited review/Special issue), *Anal. Chim. Acta*, in press.

### Invited Presentations:

- a. "Particle-based DNA Assays", ECS Meeting, San Francisco, (Sept. 2001).
- b. "Particle-based DNA Assay", Biosensors for Environmental Monitoring", Cornell University (June 2002).
- c. "Particle-based DNA Assay", European Society of Electrochemistry, Crakow, Poland (June 2002).

## **Conclusions**

Electrochemical detection of DNA hybridization offers great promise for developing fast, simple, and user-friendly DNA sensing devices for point-of-care breast-cancer testing. Our findings have already led to major improvements in the electrical

biosensing of DNA segments specific to the breast-cancer gene BRCA1. Our research has addressed the major challenges of signal amplification, non-specific (unwanted) adsorbates, and assay simplification, and should pave the way to the realization of instant point-of-care genetic testing. The realization of such decentralized DNA testing would require additional developmental work. Particular attention should be given to the major challenges of mismatch discrimination, multi-target detection, as well as integration of the DNA detection with automated sample preparation on a single microchip flow system. The signal amplification of highly-branched dendrimers is currently being combined with the remarkable mismatch discrimination of PNA oligomers. For this purpose, we are assembling PNA dendrimers involving numerous biotylated PNA attached to avidin-coated microspheres. We are also examining the coupling of dendritic amplification units (possessing numerous colloidal gold tags), with the catalytic-precipitation and enlargement of these metal tracers, and the 'built-in' preconcentration of the electrochemical stripping detection for achieving a triple-amplification bioassay.

Our effort during the last part of this project will thus focus on transforming the new electrochemical protocols into microfluidic devices. The new microsystem will rely on the use of magnetic beads not only for removing unwanted constituents, but also for localizing different probes within the microchannels. The probe-bearing beads could thus be reproducibly introduced, kept in place, manipulated, and removed/replaced after each run (in connection to a proper placement and removal of a magnet). Such reversible magnetic localization obviates the need for 'fixing' the probe onto the chips, regenerating it, and for fabricating multiple hybridization sites or special physical 'barriers', and hence would greatly simplify the fabrication and operational requirements. The new microfluidic system will thus contain multiple microstructures (functional elements) and related microchannel network for integrating various processes, including sample collection, DNA extraction, reagent mixing and amplification, with the actual hybridization detection. We have recently assembled a microfabrication laboratory that allows us to micromachine the microfluidic devices essential for such chip-based high throughput automated operation. Such user-friendly operation, on a chip platform, would allow testing for breast cancer to be performed more rapidly, inexpensively, and reliably in a decentralized setting.

## References

1. J. Wang, Chem. Eur. J. 5 (1999)1681.
2. E. Palecek and M. Fojta, Anal. Chem. 73(2001)75A.
3. J. Wang, A. Nasser, A. Erdem, M. Salazare, Analyst, 126(2001)2020.
4. J. Wang, and A. Kawde, Analyst, 127(2002)383.
5. J. Wang, D. Xu, and R. Polksky, J. Am. Chem. Soc., 124(2002)4208.
6. J. Wang and A. Kawde, Electrochemistry Communications, 4(2002)349.

## **Appendices**

Papers resulted from our second year effort (as well as those published recently as a result of the first year funding):

1. "Magnetic-beads based Label-Free Electrochemical Detection of DNA Hybridization", J. Wang, A. Nasser, A. Erdem, M. Salazare, Analyst, 126(2001)2020.
2. "Amplified Label-Free Detection of DNA Hybridization", J. Wang, and A. Kawde, Analyst, 127(2002)383.
3. "Genomagnetic Electrochemical Assays of DNA Hybridization", J. Wang, D. Xu, R. Polsky, and E. Arzum, Talanta, 56(2002)931.
4. "Magnetically-Induced Solid-State Electrochemical Detection of DNA Hybridization", J. Wang, D. Xu, and R. Polsky, J. Am. Chem. Soc., 124(2002)4208.
5. "Magnetic Field Stimulated DNA Oxidation", J. Wang and A. Kawde, Electrochemistry Communications, 4(2002)349.
6. "Metal-Nanoparticle Based Electrochemical Stripping Detection of DNA Hybridization", J. Wang, D. Xu, R. Polsky, and A. Kawde, Anal. Chem. 73(2001)5576.
7. "Silver-Enhanced Colloidal Gold Electrical Detection of DNA Hybridization", J. Wang, R. Polsky, D. Xu, Langmuir, 17(2001)5739.

---

## **Magnetically-Induced Solid-State Electrochemical Detection of DNA Hybridization**

---

**Joseph Wang, Danke Xu, and Ronen Polsky**

New Mexico State University, Department of Chemistry and  
Biochemistry, Las Cruces, New Mexico 88003

---

**JOURNAL  
OF THE  
AMERICAN  
CHEMICAL  
SOCIETY®**

---

Reprinted from  
Volume 124, Number 16, Pages 4208–4209

# Amplified label-free electrical detection of DNA hybridization

THE  
ANALYST

[www.rsc.org/analyst](http://www.rsc.org/analyst)

Joseph Wang\* and Abdel-Nasser Kawde

Department of Chemistry and Biochemistry, New Mexico State University, Las Cruces, NM 88003, USA. E-mail: [joewang@nmu.edu](mailto:joewang@nmu.edu)

Received 26th November 2001, Accepted 9th January 2002  
First published as an Advance Article on the web 8th February 2002

A new protocol is described for amplifying label-free electrochemical measurements of DNA hybridization based on the enhanced accumulation of purine nucleobases in the presence of copper ions. Such electrical DNA assays involve hybridization of the target to inosine-substituted oligonucleotide probes (captured on magnetic beads), acidic dipurination of the hybrid DNA, and adsorptive chronopotentiometric stripping measurements of the free nucleobases in the presence of copper ions. Both amplified adenine and guanine peaks can be used for detecting the DNA hybridization. The dramatic signal amplification advantage of this type of detection has been combined with efficient magnetic removal of non-complementary DNA, use of microliter sample volumes and disposable transducers. Factors influencing the signal enhancement were assessed and optimized. A detection limit of 40 fmol (250 pg) was obtained with 10 min hybridization and 5 min adsorptive-accumulation times. The advantages of this procedure were demonstrated by its application in the detection of DNA segments related to the BRCA1 breast cancer gene. The copper enhancement holds great promise not only for the detection of DNA hybridization, but also for trace measurement of nucleic acids.

## 1. Introduction

Electrochemical devices have received considerable attention in the development of sequence-specific DNA hybridization biosensors.<sup>1,2</sup> The high sensitivity of such devices, coupled to their compatibility with modern microfabrication technologies, portability, low cost (disposability), minimal power requirements, and independence of sample turbidity or optical pathway, make them excellent candidates for DNA diagnostics. Early studies have focused on the use of duplex-selective redox indicators or enzyme tags for electrical monitoring of the hybridization event.<sup>1–3</sup>

Increased attention has been given recently to label-free electrochemical detection schemes, in which the hybridization event triggers a change in an electrical signal. Label-free procedures greatly simplify the sensing protocol (as they eliminate the need for the indicator addition–association–detection steps) and offer an instantaneous detection of the duplex formation. Such label-free detection can be accomplished by monitoring changes in the intrinsic redox activity of the nucleic acid target or changes in the electrochemical properties of the interface. For example, it is possible to exploit changes in the intrinsic electroactivity of DNA (primarily the guanine oxidation) accrued from the hybridization event.<sup>4,5</sup> For this purpose, guanines in the probe sequence are substituted by inosine residues (pairing with cytosines) and the hybridization is detected through the appearance of the target DNA guanine signal. Two avenues have been successfully examined for enhancing the guanine signal, and hence hybridization response, including the electrocatalytic action of a Ru(bpy)<sub>3</sub><sup>2+</sup> redox mediator<sup>4</sup> and an adsorptive-accumulation of the hybrid coupled to a potentiometric stripping detection.<sup>5</sup>

This paper describes a new protocol for amplifying the label-free adsorptive-stripping hybridization signal based on the dramatically enhanced accumulation of purine nucleobases in the presence of copper ions. Shiraishi and Takahashi<sup>6</sup> demonstrated that the anodic response of free (monomeric) adenine and guanine is greatly enhanced in a copper solution. Taking advantage of this dramatic enhancement, the present label-free electrical protocol involves the hybridization of inosine-substituted oligonucleotide probes (captured on magnetic

beads) to the DNA target, dissociation of the hybrid DNA from the beads, an acidic dipurination, and adsorptive chronopotentiometric stripping measurements of the free nucleobases in the presence of copper ions at a disposable graphite electrode (Fig. 1). The optimization, characterization, and attractive performance characteristics of the new amplified label-free electrochemical detection of DNA hybridization are reported in the following sections in connection with the detection of

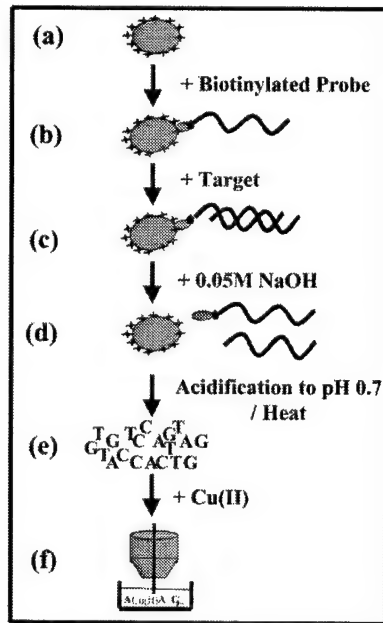


Fig. 1 Schematic representation of the analytical protocol: (a) introduction of the streptavidin-coated beads; (b) addition of the biotinylated probe (P), oligomer-immobilization event; (c) addition of the target (T), oligomer-hybridization event; (d) release of the hybrid DNA from the beads using 0.05 M NaOH solution; (e) release of the guanine and adenine bases from the DNA strands using 10 µl of a 3 M H<sub>2</sub>SO<sub>4</sub> and heating (to dryness) for 2 min; (f) potentiometric stripping detection in presence of 2 mg l<sup>-1</sup> copper.

nucleic-acid segments related to the breast-cancer BRCA1 gene.

## 2. Experimental

### 2.1 Apparatus

Chronopotentiometric measurements were performed with a potentiometric stripping unit PSU20 (Radiometer) controlled by a PC using the TAP2 software (Radiometer). The microsphere preparation and hybridization reactions were performed on a MCB 1200 Biomagnetic Processing Platform (Dexter Corporation Magnetic Technologies, Fremont, CA, USA). The three electrode system included the graphite working electrode, a Ag/AgCl reference electrode, and a platinum wire counter electrode.

### 2.2 Electrode preparation

Details of the pencil graphite electrode have been described earlier.<sup>7</sup> In brief, a pencil Model P205 (Pentel Ltd, Japan) was used as a holder for the graphite lead. The pencil graphite leads (Hi-polymer super C505) were obtained from the same source. All graphite leads had a total length of 60 mm and a diameter of 0.5 mm, and were used as received. Electrical contact to the lead was achieved by soldering a metallic wire to the metallic part that held the lead in place inside the pencil. The pencil was fixed vertically with 11 mm of the graphite rod extruding outside, 10 mm of which was immersed in the solution. This length corresponds to an active electrode area of 16.36 mm<sup>2</sup>.

### 2.3 Materials and reagents

All stock solutions were prepared using deionized and autoclaved water. Tween 20, MgSO<sub>4</sub>, and copper atomic absorption standard solution (containing 1006 µg ml<sup>-1</sup> Cu in 1 wt. % HNO<sub>3</sub>) were purchased from Aldrich. Sodium acetate buffer (3M, pH 5.2), Tris-HCl buffer, CH<sub>3</sub>COONa·3H<sub>2</sub>O, glacial CH<sub>3</sub>COOH, LiCl, NaOH and NaCl were purchased from Sigma. Proactive streptavidin-coated microspheres (CMO1N-lot 5205) were purchased from Bangs Laboratories (Fishers, IN, USA).

Single-stranded calf thymus DNA (ssDNA, lyophilized powder, Cat. No. D-8899), adenine (Cat. No. A-8626) and guanine (Cat. No. G-6779) were used as received from Sigma (St. Louis, MO, USA).

Oligonucleotides (with and without 5'-biotin modification) were acquired from Life Technologies Inc. (Grand Island, NY, USA), and had the following sequences:

*Immobilized probe*, biotinylated inosine-substituted E908X-WT: biotin-5' IAT TTT CTT CCT TTT ITT C

*Target*, E908X-WT: 5'-GAA CAA AAG GAA GAA AAT C

*Non-complementary strand*, E908X: 5'-GGT CAG GTG GGG GGT ACG CCA GG.

### 2.4 Preparation of the oligomer-coated microspheres and analytical procedure

The bead preparation (performed on the MCB 1200 Biomagnetic Processing Platform) was carried out using a modified procedure recommended by Bangs Laboratories.<sup>8</sup> Briefly, 100 µg of streptavidin-coated microspheres (Fig. 1a) were transferred into a 1.5 ml centrifuge tube. The microspheres were washed with 100 µl TTL buffer (100 mM Tris-HCl, pH 8.0, and 0.1 % Tween 20 and 1M LiCl) and resuspended in 21 µl TTL

buffer. The oligomer probe, 5 µg, was added and incubated for 15 min at room temperature with gentle mixing. The immobilized probe (Fig. 1b) was then separated, rinsed twice with 100 µl TT buffer (250 mM Tris-HCl, pH 8.0, and 0.1% Tween 20), and resuspended in the 50 µl hybridization solution (750 mM NaCl and 75 mM sodium citrate). The desired amount of the target was subsequently spiked. The hybridization reaction was carried out for 10 min at room temperature. The resulting hybrid-conjugated microspheres (Fig. 1c) were then washed with 100 µl acetate buffer (0.2 M, pH 5) and resuspended in 50 µl 0.05 M NaOH solution. After a 5 min mixing step (Fig. 1d) and a subsequent magnetic separation, the 50 µl NaOH solution (containing the denatured oligomer DNA) was transferred into the 'acid-digestion' cell. It was then spiked with 10 µl of a 3M sulfuric acid solution, and was heated till dryness (Fig. 1e). An acetate buffer solution (1 ml, 0.5 M, pH 5.9) was used to transfer the digested DNA into the detection cell. The solution was spiked with 2 mg l<sup>-1</sup> copper(II) prior to the electrochemical measurement (final pH, 4.8).

Chronopotentiometric adsorptive-stripping measurements of the released guanine and adenine nucleobases were performed using a 'fresh' 10 mm long graphite lead (without any surface pretreatment) and a 2 min accumulation at -0.05 V (from the sample-containing stirred acetate buffer solution). Subsequent stripping was performed after a 5 s rest period (without stirring) using an applied oxidative current of +2.0 µA. The stripping curve data were filtered and baseline corrected using the TAP2 software.

## 3. Results and discussion

### 3.1 Measurements of nucleic acids

Shiraishi and Takahashi<sup>6</sup> reported on the enhanced voltammetric response of free (monomeric) guanine and adenine nucleobases in the presence of copper, and attributed their observation to accumulation of the copper(I)-purine complex. In the present work we examine this signal enhancement in connection to trace measurements of nucleic acids and exploit it for amplifying the label-free detection of DNA hybridization. The adaptation of this amplification route for nucleic acid analysis requires a rapid (acidic) release of the purine bases bound in the polynucleotide.

Fig. 2 compares cyclic voltammograms at the graphite electrode for a 15 mg l<sup>-1</sup> ssDNA solution, following an adsorptive accumulation of the nucleic acid (a), and by coupling such accumulation to an acid treatment (b), as well as to

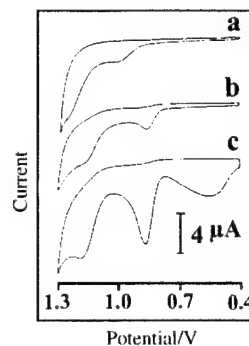


Fig. 2 Cyclic voltammograms for (a) 15 mg l<sup>-1</sup> ssDNA solution, (b) same as (a) but following 'acid-digestion' of the ssDNA; (c) as (b) but in the presence of 2 mg l<sup>-1</sup> Cu(II). Acetate buffer solution (1 ml); (a) 0.2 M, pH 5.0; (b,c) 0.5 M, pH 5.9; a graphite pencil electrode (with a 10 mm long HB lead). Pretreatment at +1.4 V for 1 min (a). Accumulation for 1 min at +0.5 V (a), and at -0.05 V (b,c) under stirred conditions. Scan rate, 50 mV s<sup>-1</sup>.

complexation of the purine bases with copper (c). In accordance with early studies<sup>9–11</sup> the adsorptive accumulation results in small anodic peaks (at 1.05 and 1.25 V), corresponding to the oxidation of the bound guanine and adenine, respectively (a). These peaks increase following the acid treatment and shift to lower potentials of 0.87 (guanine) and 1.18 V (adenine), reflecting the behavior of the free (monomeric) nucleobases.<sup>12</sup> A substantial enhancement of both peaks is observed in the presence of copper ions (c). The peak potentials remain unchanged, and a new and broad copper-oxidation peak appears around +0.55 V. Despite the copper enhancement, the adenine peak is poorly defined due to the rising solvent-decomposition background current. Note that while the same initial potential was employed, different accumulation potentials were employed prior to the scan (in accordance with the optimal adsorptive behavior discussed below).

Such background contributions can be readily addressed by using a chronopotentiometric (PSA) operation.<sup>10,11</sup> Fig. 3 displays PSA signals for ssDNA under conditions analogous to those used for attaining the voltammetric response of Fig. 2. The sophisticated baseline correction capability of the computerized PSA operation results in a flat background, and offers convenient quantitation of both (the bound and free) purine nucleobases. A small bound-guanine peak was observed following the 1 min adsorptive accumulation (A), whereas two well-defined PSA peaks were observed following the acid treatment (B). These adenine (a) and guanine (b) peaks greatly increase in the presence of copper ions (C).

Various parameters affecting the enhancement of the purine response have been examined and optimized. Fig. 4 shows the influence of the accumulation time (A) and potential (B), as well as the copper concentration (C) upon the PSA response to a mixture containing 1 mg l<sup>-1</sup> of free adenine (O) and guanine (●) nucleobases. The signals of both purine bases increase rapidly and linearly with adsorption time up to 2 min, they then slow down, and start to level off above 6–7 min (A). The potential dependence (B) exhibits peak-shaped profiles, with the response of both purines increasing rapidly between -0.55 V to -0.1 V, then more slowly (with a maximum around -0.05 V), with a rapid decrease above 0.0 V. Such profiles reflect the

redox chemistry of copper, with the reduction to copper(I) (participating in the purine complexation) occurring around 0.0 V (vs. SCE).<sup>6</sup> This is in contrast to a potential of +0.5V which is optimal for the adsorptive accumulation of nucleic acids (without copper).<sup>10,11</sup> No surface pretreatment was required for facilitating the adsorption of the copper-purine complexes (as compared to an electrochemical activation common for analogous measurements based on the adsorption of nucleic acids).<sup>5,10,11</sup> A linear dependence is observed between the adenine and guanine response and the copper(II) concentration up to 2 mg l<sup>-1</sup>, with a slight curvature at higher copper levels (C). These profiles reflect the dramatic copper-based signal enhancement, e.g., ca. 16- and 31-fold increase of the guanine peak in the presence of 2 and 4 mg l<sup>-1</sup> copper, respectively (vs. the response without copper). Most subsequent work employed accumulation at -0.05 V for 2 min, along with a copper concentration of 2 mg l<sup>-1</sup> (in combination with 3M sulfuric acid and heating to facilitate the dipurinazation). A similar copper enhancement, and favorable signal-to-background characteristics were observed at the glassy-carbon, carbon-paste, and graphite pencil electrodes. The latter was used throughout due to its low cost, disposability, and convenience of operation.

### 3.2 Detection of DNA hybridization

The use of the amplified purine response for detecting DNA hybridization was illustrated for the detection of DNA segments related to the BRCA1 breast cancer gene. Fig. 5 compares the stripping response for 2 mg l<sup>-1</sup> DNA target, obtained by using conventional guanine detection (A), after an acid dipurinazation (B(a)) and by combining the acid treatment in the presence of copper ions (B(b)). The former yields a small guanine oxidation peak ( $E_p = 1.04$  V; area = 12.5 ms). Two well-defined adenine and guanine peaks are observed following the acidification step (B(a)). These peaks are greatly enhanced following the copper addition (B(b)). For example, the resulting guanine peak has an area of 305 ms, that is 25 times greater than that observed by the traditional stripping detection (A vs. B(b)); note the different scales). While both purine peaks can be used for detecting the hybridization event, the guanine peak is preferred due to its higher precision and smaller background (associated with the use of guanine-free probes and a lower detection potential). Substantially smaller signals are observed for a 100-fold excess (200 mg l<sup>-1</sup>) of non-complementary DNA (B(c)), reflecting the efficient magnetic removal of non-hybridized DNA (i.e., elimination of various sample matrix effects).<sup>5</sup>

Fig. 6 displays the dependence of the response upon the concentration of the breast cancer DNA target. The peak area increases rapidly with the target concentration at first (up to 5 mg l<sup>-1</sup>), then more slowly, and starts to level off above 15 mg l<sup>-1</sup>. Such curvature reflects the saturation of the probe hybridization sites, as well as of surface (adsorption) sites. Also shown in Fig. 6 (inset) is the actual chronopotentiometric signal to a 0.2 mg l<sup>-1</sup> target concentration (using a 5 min accumulation). Such response (0.42 s V<sup>-1</sup>), along with the corresponding noise level (0.004 s V<sup>-1</sup>), indicates a detection limit of 5 µg l<sup>-1</sup>.

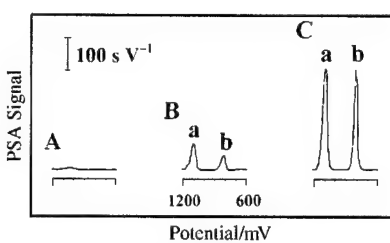


Fig. 3 Stripping potentiograms for (A) 15 mg l<sup>-1</sup> ssDNA solution, (B) same as (A) but after 'acid-digestion' of the ssDNA; (C) as (B) but in the presence of 2 mg l<sup>-1</sup> Cu(II). Acetate buffer solution (1 M; (A) 0.2 M, pH 5.0; (B,C) 0.5 M, pH 5.9) using a graphite pencil electrode pretreated at +1.4 V for 1 min (A). Accumulation at +0.5 (A) and at -0.05 (B,C) V for 1 min under stirred conditions. Stripping was performed in a quiescent solution using a constant current of +5 µA (A) and +2 µA (B,C).

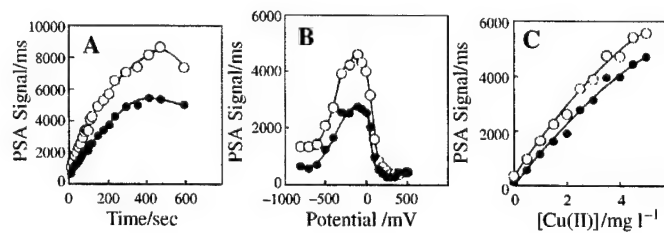
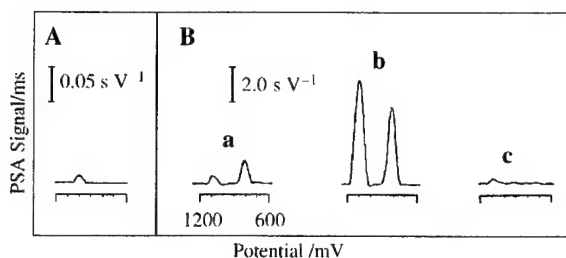
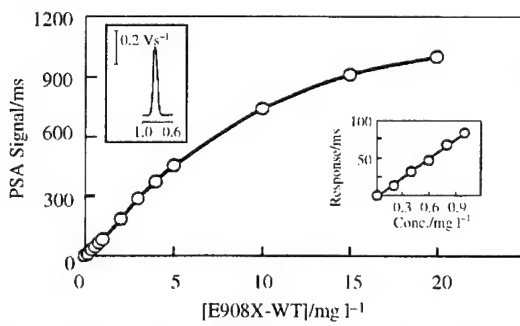


Fig. 4 Effect of the accumulation time (A), accumulation potential (B), and copper concentration (C) upon the potentiometric stripping detection of a mixture containing 1 mg l<sup>-1</sup> adenine (O), 1 mg l<sup>-1</sup> guanine (●), in 2 ml of acetate buffer solution (0.2 M, pH 5.0); copper concentration, 4 mg l<sup>-1</sup> (A,B); stripping current; +5 µA: (A) accumulation potential, +0.05V; (B) accumulation time, 30 s; (C) accumulation at -0.05 V for 120 s.

(i.e., 0.8 nM) in connection with the 10 min hybridization time (based on S/N = 3). This detection limit corresponds to 250 pg (40 fmol) in the 50  $\mu$ l samples. Analogous ‘copper-free’ stripping hybridization measurements yielded a detection limit of 100  $\mu$ g l<sup>-1</sup> (5 ng).<sup>5</sup> Further lowering of the detection limit is expected when longer targets, longer hybridization time or deposition periods are used. A series of 6 repetitive measurements of the 4 mg l<sup>-1</sup> target solution was used for estimating the precision (10 min hybridization; not shown). This series yielded a mean guanine peak area of 432 ms and a relative standard deviation of 6%.



**Fig. 5** Chronopotentiometric stripping hybridization signals to 2 mg l<sup>-1</sup> undigested E908X-WT target (A), 2 mg l<sup>-1</sup> digested E908X-WT target (B(a)), 2 mg l<sup>-1</sup> digested E908X-WT target in presence of 2 mg l<sup>-1</sup> Cu(II) (B(b)), 200 mg l<sup>-1</sup> digested non-complementary (NC) oligomer in presence of 2 mg l<sup>-1</sup> Cu(II), (B(c)). Amount of beads, 100  $\mu$ g; probe concentration, 200 mg l<sup>-1</sup>; hybridization time, 10 min; accumulation potential, +0.5 V (A), and -0.05 V (B); accumulation time, 2 min; stripping current, +5  $\mu$ A (A), and +2  $\mu$ A (B). Other conditions, as in Fig. 3.



**Fig. 6** Calibration plot for digested E908X-WT target in presence of 2 mg l<sup>-1</sup> Cu(II). Accumulation for 2 min at -0.05 V; stripping current, +2  $\mu$ A. One inset shows a portion of the curve covering the low 0.2–1.0 mg l<sup>-1</sup> range. The second inset displays the actual response for a 0.2 mg l<sup>-1</sup> E908X-WT target using a 5 min accumulation. Other conditions, as in Fig. 5 (B(c)).

In conclusion, we have described a novel route for amplifying label-free electrochemical detection of DNA hybridization based on the greatly enhanced anodic stripping signals of the purine nucleobases in the presence of copper ions. The dramatic signal amplification advantage of the new label-free stripping detection has been combined with an efficient magnetic removal of non-complementary DNA, use of microliter sample volumes and of disposable transducers. Such effective magnetic isolation can address the effect of other unwanted co-existing constituents, including copper-complexing compounds and unbound nucleoside residues. Such attractive performance characteristics, along with the elimination of reporter molecules, offer great promise for centralized and decentralized genetic testing. Further improvements (towards the detection of point mutations) are expected by coupling the copper-enhanced label-free assay with the use of PNA probes. In addition to detecting DNA hybridization, the greatly enhanced purine signals can benefit ultratrace measurements of various nucleic acids, and the detection of the purine content in DNA and RNA samples (including estimates of the guanine:adenine ratio).

### Acknowledgment

This work was supported by the National Institutes of Health (Grant No. R01 14549-02) and US Army Medical Research (Award No. DAMD17-00-1-0366). A.K. acknowledges a fellowship from the Egyptian government.

### References

- 1 J. Wang, *Chem. Eur. J.*, 1999, **5**, 1681.
- 2 E. Palecek and M. Fojta, *Anal. Chem.*, 2001, **73**, 75A.
- 3 S. R. Mikkelsen, *Electroanalysis*, 1996, **8**, 15.
- 4 D. H. Johnston, K. Glasgow and H. H. Thorp, *J. Am. Chem. Soc.*, 1995, **117**, 8933.
- 5 J. Wang, A. Kawde, A. Erdem and M. Salazare, *Analyst*, 2001, **126**, 2020.
- 6 H. Shiraishi and R. Takahashi, *Bioelectrochem. Bioenerg.*, 1993, **31**, 203.
- 7 J. Wang, A. Kawde and E. Sahlin, *Analyst*, 2000, **125**, 5.
- 8 Technote 101, Bangs Laboratories Inc., Fishers, IN.
- 9 E. Palecek, *Electroanalysis*, 1996, **8**, 7.
- 10 J. Wang, X. Cai, C. Jonsson and M. Balakrishnan, *Electroanalysis*, 1996, **8**, 20.
- 11 J. Wang, X. Cai, J. Wang, C. Jonsson and E. Palecek, *Anal. Chem.*, 1995, **66**, 4065.
- 12 V. Brabec and J. Koudelka, *Bioelectrochem. Bioenerg.*, 1980, **7**, 793.

# Magnetic bead-based label-free electrochemical detection of DNA hybridization

Joseph Wang,\* Abdel-Nasser Kawde, Arzum Erdem† and Marcos Salazar

Department of Chemistry and Biochemistry, New Mexico State University, Las Cruces, NM 88003, USA. E-mail: joewang@nmsu.edu

Received 17th July 2001, Accepted 24th August 2001  
First published as an Advance Article on the web 22nd October 2001

Magnetic bead capture has been used for eliminating non-specific adsorption effects hampering label-free detection of DNA hybridization based on stripping potentiometric measurements of the target guanine at graphite electrodes. In particular, the efficient magnetic separation has been extremely useful for discriminating against unwanted constituents, including a large excess of co-existing mismatched and non-complementary oligomers, chromosomal DNA, RNA and proteins. The new protocol involves the attachment of biotinylated oligonucleotide probes onto streptavidin-coated magnetic beads, followed by the hybridization event, dissociation of the DNA hybrid from the beads, and potentiometric stripping measurements at a renewable graphite pencil electrode. Such coupling of magnetic hybridization surfaces with renewable graphite electrode transducers and label-free electrical detection results in a greatly simplified protocol and offers great promise for centralized and decentralized genetic testing. A new magnetic carbon-paste transducer, combining the solution-phase magnetic separation with an instantaneous magnetic collection of the bead-captured hybrid, is also described. The characterization, optimization and advantages of the genomagnetic label-free electrical protocol are illustrated below for assays of DNA sequences related to the breast-cancer BRCA1 gene.

## Introduction

Biosensing devices, combining the base-pair recognition of DNA probes with the advantages of electrochemical transducers are currently receiving enormous attention.<sup>1–3</sup> Recent activity has led to powerful, elegant, and highly sensitive protocols for the detection of specific DNA sequences.<sup>1–10</sup> Electrochemical devices are also uniquely qualified for meeting the minimal size, cost, and power requirements of decentralized DNA testing.<sup>2,11</sup> Most electrochemical avenues for detecting DNA hybridization make use of duplex-specific redox indicators<sup>1,5,7</sup> or enzyme tags that are captured following the hybridization.<sup>6,8</sup> However, there are potential advantages of simplicity and speed for detecting the hybridization step directly without using such labels. Particularly attractive are label-free gene-sensing schemes based on the intrinsic electroactivity of DNA.<sup>9,12</sup> These methods have relied primarily on monitoring changes in the guanine oxidation process accrued from the hybridization event.

A major problem with these label-free operations, as well as in all electrochemical DNA transduction routes, is the non-specific adsorption of non-hybridized nucleic acids and of other surface-active co-existing molecules. For example, an excess of non-complementary oligonucleotides often results in the appearance of a guanine oxidation peak in connection with the use of guanine-free (inosine-substituted) probes.<sup>12</sup> The minimization of these non-specific adsorption effects requires sophisticated surface modification schemes for controlling the surface architecture (particularly the use of mixed oligonucleotide–‘blocking’ layer).<sup>13</sup>

In this article we report on the coupling of the label-free guanine detection route with an efficient magnetic isolation of the hybrid for addressing the non-specific adsorption problem. Magnetic bead capture constitutes a powerful tool for bio-affinity assays,<sup>14</sup> but has rarely been used for electrical

detection of DNA hybridization. Recent work in our laboratory<sup>15</sup> and that of Palecek *et al.*<sup>16</sup> has illustrated that major errors associated with non-specific adsorption can be eliminated by conducting the hybridization and transduction steps at different surfaces (magnetic beads and unmodified electrodes, respectively). Such substantial improvements in the reliability have been demonstrated in connection with enzyme-linked sandwich hybridization assays<sup>15</sup> and cathodic-stripping or catalytic-voltammetric measurements at mercury electrodes.<sup>16</sup>

The present biomagnetic assay format (illustrated in Fig. 1) involves: (a) capture of inosine-substituted (guanine-free) probes on streptavidin-coated magnetic spheres; (b) the hybridization event and magnetic removal of non-hybridized oligonucleotides; (c) alkaline treatment (releasing the hybrid from the spheres and denaturing it); and (d) subsequent adsorptive stripping chronopotentiometric detection of the target guanine oxidation peak at a renewable graphite (pencil) electrode. The magnetic isolation of the DNA hybrid has been accomplished using a biomagnetic processing technology, combining low-volume magnetic mixing and separation.<sup>17</sup> The coupling of magnetic hybridization surfaces with renewable transducers and label-free electrical detection eliminates the need for a regeneration step, advanced surface modification schemes and an external indicator, and results in a greatly simplified protocol. Further simplification of the assay is accomplished by eliminating the alkaline treatment and adsorptive-accumulation steps in connection to magnetic ‘collection’ of bead-captured hybrid at a new magnetic carbon-paste electrode. The characterization and optimization of the resulting genomagnetic label-free electrical protocols are illustrated below for assays of DNA sequences related to the BRCA1 breast-cancer gene.<sup>18</sup>

## Experimental

### Apparatus

Chronopotentiometric measurements were performed with a potentiometric stripping unit PSU20 (Radiometer) in connec-

† On leave from Ege University, Faculty of Pharmacy, Analytical Chemistry Department, 35100 Bornova-Izmir, Turkey.

tion to the TAP2 software (Radiometer). The three-electrode system consisted of the carbon working electrode, an Ag/AgCl (BAS RE-1) reference electrode and a platinum wire counter electrode. The three electrodes joined the 1 ml electrochemical cell through holes in its Teflon cover. Microsphere preparation and hybridization reactions were performed on a MCB 1200 biomagnetic processing platform (Dexter Corporation Magnetic Technologies, Fremont, CA, USA).<sup>17</sup>

### Electrode preparation

Details of the renewable pencil graphite electrode transducer, used in most experiments, were described earlier.<sup>19</sup> A Pentel pencil Model P205 (Japan) was used as a holder for the graphite lead. Electrical contact with the lead was obtained by soldering a metallic wire to the metallic part (holding the lead in place inside the pencil). The pencil was fixed vertically with 11 mm of the lead extruded outside (10 mm of which was immersed in the solution). Such length corresponds to an active electrode area of 16.36 mm<sup>2</sup>.

Several experiments were conducted with a magnetic carbon-paste electrode. This involved a Teflon body with a 3.5 mm id cavity containing a small magnet and a tightly packed carbon paste. The electrical contact was made with a copper wire. The carbon paste was prepared in the usual way by hand-mixing graphite powder and mineral oil (using a graphite powder/mineral oil ratio of 70:30).

### Materials and reagents

All stock solutions were prepared using deionized and autoclaved water. Tween 20, and MgSO<sub>4</sub> were purchased from Aldrich. Sodium acetate buffer (pH 5.2, 3 M at 25 °C), TRIS-HCl buffer, LiCl, Na<sub>2</sub>EDTA, NaOH and NaCl were purchased from Sigma. Proactive streptavidin-coated microspheres (CMO1N-lot 4725) were purchased from Bangs Laboratories. Pencil graphite leads, Hi-polymer super C505 (black lead) of

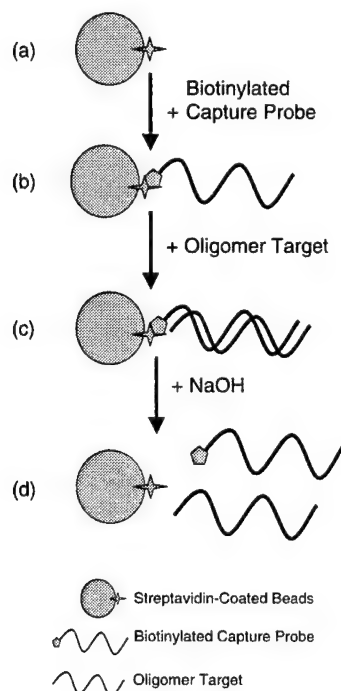


**Fig. 1** Schematic representation of the analytical protocol: (a) introduction of the streptavidin-coated beads; (b) magnetic capture of the biotinylated probe; (c) hybridization event; (d) release of hybrid DNA from the beads using 0.05 M NaOH solution.

type HB, were obtained from Pentel Co. Ltd. (Japan). All graphite leads have a total length of 60 mm and a diameter of 0.5 mm.

The following biochemicals were used as received from Sigma (St. Louis, MO, USA): single-stranded calf thymus DNA (ssDNA, lyophilized powder, Cat. No. D-8899), transfer RNA (tRNA, from baker's yeast, lyophilized powder, Cat. No. R-8759), and bovine albumin (Cat. No. A-7906).

Oligonucleotides (with and without 5'-biotin modification) were acquired from Life Technologies (Grand Island, NY, USA) and had the following sequences: Immobilized probe: biotinylated inosine-substituted E908X-WT; biotin-5' IAT TTT CCT CCT TTT ITT C. Immobilized probe: biotinylated E908X-WT; biotin-5' GAT TTT CCT CCT TTT GTT C. Target (I): E908X-WT; 5'-GAA CAA AAG GAA GAA AAT C. Target (II): 5'-GAA CAA AAG GAA GAA AAT CGA ACA AAA GGA AGA AAA TCC TAA AAG AAG GAA AAC AAG. Non-complementary strand: E908X; 5'-GGT CAG GTG GGG GGT ACG CCA GG. Mismatched strand: E908X-WT (3 bm); 5'-CAA CAA AAG CAA CAA AAT C.

### Preparation of oligomer-coated microspheres and analytical procedure

The bead preparation (performed on the MCB 1200 biomagnetic processing platform) was carried out using a modified procedure recommended by Bangs Laboratories (Technical Note 101). Usually, 70 µg of the streptavidin-coated microspheres (Fig. 1a) were transferred into a 1.5 ml centrifuge tube. The microspheres were washed with 100 µl TTL buffer (100 mM TRIS-HCl, pH 8.0, 0.1% Tween 20 and 1 M LiCl) and resuspended in 21 µl TTL buffer. Then, 5 µg of the oligonucleotide probe were added and incubated for 15 min at room temperature with gentle mixing. The bead-captured probes (Fig. 1b) were then separated, and washed twice with 100 µl TT buffer (250 mM TRIS-HCl, pH 8.0, and 0.1% Tween 20), and resuspended in 50 µl hybridization solution (750 mM NaCl and 75 mM sodium citrate) containing the desired amount of the DNA target. The hybridization reaction usually proceeded for 10 min at room temperature. The hybrid-conjugated beads (Fig. 1c) were then washed twice with 100 µl acetate buffer (0.2 M, pH 5) and resuspended in 50 µl 0.05 M NaOH solution. A 5 min magnetic mixing (step mode) was followed by magnetic isolation of the beads, and transfer of the 50 µl NaOH solution (containing the dissociated oligomers) to the electrochemical cell containing 950 µl acetate buffer (0.2 M, pH 5) supporting electrolyte solution.

### Chronopotentiometric adsorptive stripping analysis

Each measurement was performed using a new 10-mm long graphite lead. The stripping protocol involved pretreatment of the surface at +1.4 V for 1 min, followed by 1 min accumulation time at +0.5 V in a stirred solution of acetate buffer solution (0.2 M, pH 5). Subsequent stripping was carried out in a quiescent solution after a 5 s rest period by applying an anodic current of +5.0 µA. The stripping data were filtered and baseline corrected with the TAP2 software. Some experiments employed a magnetic carbon-paste electrode for collecting the bead-captured hybrids (without alkaline treatment and adsorptive accumulation).

### Results and discussion

The new stripping potentiometric genomagnetic protocol couples the analytical advantages of label-free chronopotentiometric guanine detection with the efficient separation of the magnetic bead capture. In particular, the application of

magnetic beads successfully addresses non-specific adsorption effects hampering this and other electrical protocols and hence substantially improves the assay reliability.

Such improvements are demonstrated in Fig. 2. The flat baseline over the +0.6 to +1.2 V range (A) reflects the power of computerized chronopotentiometry to address the large background contributions characterizing graphite (and other solid) electrodes at extreme potentials around the guanine oxidation. Such effective background correction leads to a well-defined hybridization signal (B). A sharp anodic peak ( $E_p = +1.06$  V), corresponding to the target guanine is observed following a 5 min hybridization. In contrast, negligible signals are observed for large excess of non-complementary and mismatched oligonucleotides (C and D, respectively). The mixture response of Fig. 2E also reflects the effective discrimination against excess of unwanted constituents. A large (10-fold excess) of the non-complementary oligomer has a negligible effect upon the target response (compare A and B).

Other potential interferences can also be eliminated by the efficient separation of the magnetic bead capture. For example, Fig. 3 displays that the DNA hybridization response (A) is not influenced by the presence of a large (25-fold) excess of chromosomal DNA (B), tRNA (C) or bovine albumin (D). While such surface-active nucleic acids or protein commonly compete for surface sites and strongly influence adsorptive stripping measurements, they are effectively removed by the magnetic separation and have a negligible effect upon the target hybridization signal (A vs. B–D).

Since the new genomagnetic electrical assay relies on adsorptive-stripping potentiometric detection of the target (released by the alkaline treatment; Fig. 1d), it is essential to examine and optimize relevant experimental parameters. The dependence of the stripping response on the deposition potential was examined over the +0.1 to +0.9 V range (Fig. 4A). The response rises gradually between +0.1 and +0.5 V and decreases slowly between +0.5 and +0.9 V. The effect of the accumulation time upon the stripping signal is shown in Fig. 4B. The peak area increases rapidly with accumulation time up to 60 s, then

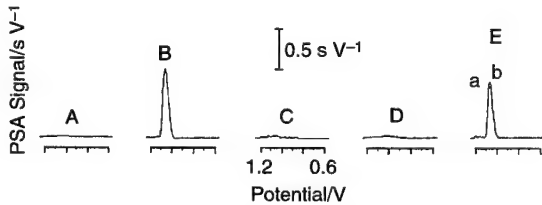


**Fig. 2** Chronopotentiometric stripping hybridization response to: (A) the blank solution; (B)  $20 \text{ mg l}^{-1}$  ( $\mu\text{g ml}^{-1}$ ) 19 bp long target T; (C)  $100 \text{ mg l}^{-1}$  non-complementary (NC) oligomer; (D)  $50 \text{ mg l}^{-1}$  three-base mismatched oligomer; (E, a) a mixture of  $15 \text{ mg l}^{-1}$  T and  $150 \text{ mg l}^{-1}$  NC;  $15 \text{ mg l}^{-1}$  T; (E, b) amount of beads,  $100 \mu\text{g}$ ; probe concentration,  $200 \text{ mg l}^{-1}$ ; hybridization time, 5 min; stripping current,  $+5.0 \mu\text{A}$ ; accumulation potential  $+0.5 \text{ V}$  for 1 min. Graphite (pencil) electrode pretreated at  $+1.4 \text{ V}$  for 1 min.

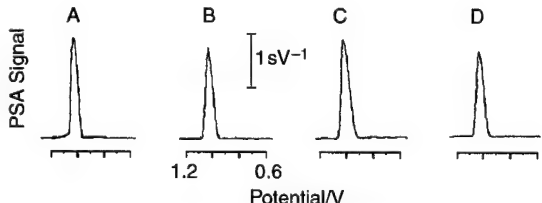


**Fig. 3** Chronopotentiometric stripping hybridization signal to  $20 \text{ mg l}^{-1}$  19 bp-long target (A), a mixture of  $20 \text{ mg l}^{-1}$  T and  $500 \text{ mg l}^{-1}$  ssDNA (B), a mixture of  $20 \text{ mg l}^{-1}$  T and  $500 \text{ mg l}^{-1}$  tRNA (C) and a mixture of  $20 \text{ mg l}^{-1}$  T and  $500 \text{ mg l}^{-1}$  albumin (D). The beads amount,  $100 \mu\text{g}$ ; probe concentration,  $200 \text{ mg l}^{-1}$ ; adsorptive accumulation time, 2 min. Other conditions, as in Fig. 2.

more slowly, and levels off above 120 s. The response decreases gradually upon increasing the stripping current between  $+5$  and  $+10 \mu\text{A}$ , then more slowly, and levels off above  $+15 \mu\text{A}$  (Fig. 4C). Most subsequent work thus employed a 1 min accumulation time at  $+0.5 \text{ V}$  in connection to a stripping current of  $+5 \mu\text{A}$ .

The amount of the magnetic beads has a profound effect upon the sensitivity of the new genomagnetic label-free protocol (Fig. 5A). The hybridization guanine signal increases rapidly and nearly linearly between  $20$  and  $60 \mu\text{g}$ , then more slowly, and levels off above  $100 \mu\text{g}$ . Subsequent work employed  $100 \mu\text{g}$  beads which corresponded to  $1.9 \mu\text{g}$  captured probe (based on the  $19 \mu\text{g}$  biotinylated-probe per  $1 \text{ mg}$  binding capacity of the spheres). An excess amount of the probe ( $4 \mu\text{g}$ ) was used to ensure a full surface coverage. Fig. 5B evaluates the effect of the hybridization time upon the stripping signal. The response

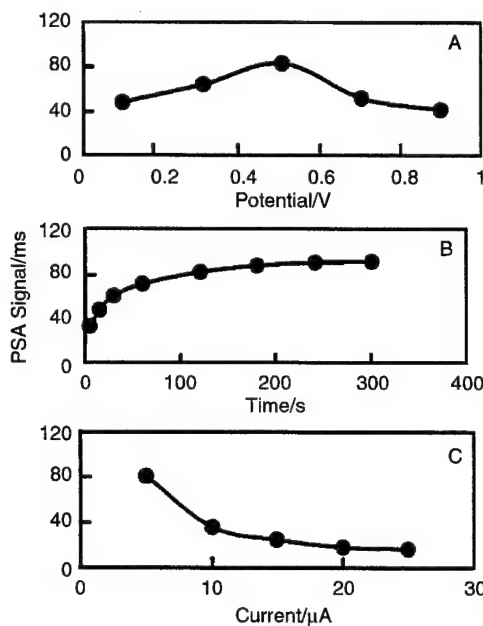


**Fig. 4** Effect of the deposition potential (A), accumulation time (B), and stripping current (C) upon the potentiometric stripping response for  $1 \text{ mg l}^{-1}$  of the  $19 \text{ bp}$ -long E908X-WT oligonucleotide. (A) Accumulation time, 1 min; stripping current,  $+5.0 \mu\text{A}$ ; (B) deposition potential,  $+0.5 \text{ V}$ ; stripping current,  $+5.0 \mu\text{A}$ ; (C) deposition potential  $+0.5 \text{ V}$  for 1 min.

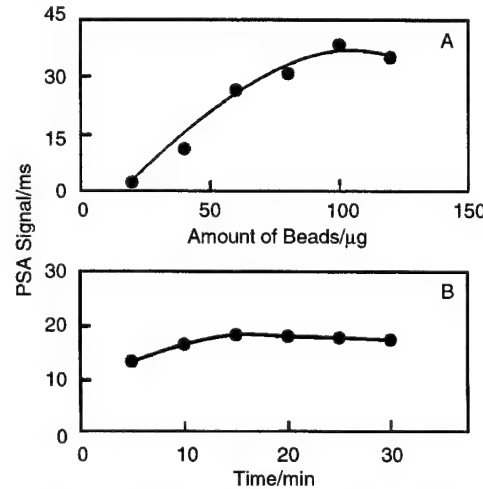


**Fig. 5** (A) Effect of the amount of streptavidin-coated microspheres; target concentration,  $20 \text{ mg l}^{-1}$ . (B) Influence of the hybridization time. Amount of magnetic beads,  $70 \mu\text{g}$ ; probe concentration,  $200 \text{ mg l}^{-1}$ ;  $19 \text{ bp}$ -long target concentration,  $10 \text{ mg l}^{-1}$ . Other conditions, as in Fig. 2.

increases slowly with the hybridization time up to 15 min, and levels off above 20 min.

The quantitative behavior was assessed by monitoring the dependence of the hybridization guanine peak area upon the concentration of the breast-cancer oligonucleotide target. Typical calibration data are displayed in Fig. 6. As expected for inosine-substituted probes, a flat baseline is observed in the absence of target DNA (a). Well-defined hybridization signals are observed over the  $1\text{--}30 \mu\text{g ml}^{-1}$  range in connection to a 10 min hybridization period (b–k). The response increases linearly with the target concentration up to  $10 \mu\text{g ml}^{-1}$ , then more slowly, and levels off above  $20 \mu\text{g ml}^{-1}$ . The initial linear portion has a slope of  $5.53 \text{ mg } \mu\text{g}^{-1}$ . Analogous measurements of a  $500 \text{ ng ml}^{-1}$  target solution were used to estimate the detection limit (not shown). A value of around  $100 \text{ ng ml}^{-1}$  was thus estimated based on the signal-to-noise characteristics of these data ( $S/N = 3$ ). Such detection limit corresponds to  $5 \text{ ng}$  in the  $50 \mu\text{l}$  samples (*i.e.*,  $160 \text{ pM}$ ). While longer hybridization times or long DNA targets are expected to further lower the detection limit, the present protocol would still require coupling with a PCR amplification for meeting the demands of real-life applications.

A series of six repetitive measurements of the  $20 \mu\text{g ml}^{-1}$  breast-cancer gene target solution was used for estimating the precision (5 min hybridization time; not shown). This series yielded a mean peak area of  $25 \text{ ms}$  and a relative standard deviation of 12%. Such reproducibility was obtained in connection to a simple and fast surface renewal inherent to pencil electrode transducers.<sup>19</sup> The coupling of such renewable transducers with magnetic hybridization surfaces and the label-free electrical detection results in a greatly simplified protocol.

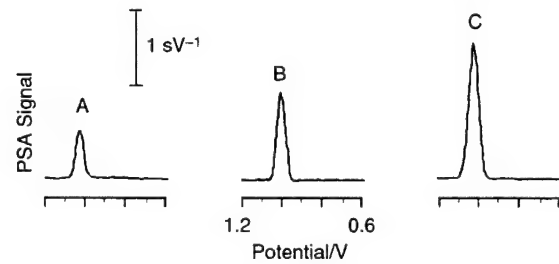
It is also possible to use short oligonucleotide probes (containing few guanine nucleobases), in connection to the detection of long DNA target (containing numerous guanines) and to follow the hybridization event from the increased guanine signal. Fig. 7 shows the chronopotentiometric hybridization response for different levels of a 57 bp long target (B, C), along with the corresponding background signal (A). While this protocol results in a small background response (compared to the flat baseline observed with inosine-substituted probes; *e.g.* Fig. 2A and 6a), well defined increasing signals are observed for increasing target concentrations. Longer targets ( $> 100 \text{ bp}$ ) are thus expected to offer substantially higher sensitivity in connection to a small and constant background signal. The background signal (of Fig. 7A) indicates that the alkaline treatment (Fig. 1d) not only denatures the DNA hybrid, but also

dissociates the streptavidin–biotin bond. Such release of the nucleic acid from the magnetic beads is essential for performing the adsorptive stripping detection (involving magnetic stirring during the accumulation step). Such adsorptive stripping detection is influenced by the number of guanines, their location (*i.e.*, the sequence), the oligonucleotide length, and surface roughness/accessibility.<sup>20</sup> Note also that the use of guanine-containing probes results in a stronger (G–C) hybridization compared to the corresponding I–C one. While regenerating ‘probe-free’ magnetic beads, the alkaline treatment also affects the streptavidin binding sites (to prevent effective reuse of these spheres).

It is possible to also avoid the alkaline treatment and stirring/accumulation steps by ‘collecting’ the bead-captured hybrid onto a new magnetic electrode transducer. In particular, a magnet can be readily placed within the cavity of carbon-paste transducers (widely used for detecting DNA guanine oxidation;<sup>21</sup> see inset of Fig. 8). Combining the solution-phase magnetic separation (described above) with the interfacial magnetic ‘collection’ of the hybrid results in a remarkable discrimination against unwanted constituents. Fig. 8 displays stripping signals (following a 10 min hybridization) obtained with the magnetic carbon-paste electrode for a  $5 \mu\text{g ml}^{-1}$  target (a),  $50 \mu\text{g ml}^{-1}$  mismatched (b), and  $150 \mu\text{g ml}^{-1}$  non-complementary (c) oligonucleotide solutions. The magnetic transducer exhibits a well-defined chronopotentiometric target signal, but a negligible response to the 10- and 30-fold excess of the mismatched and non-complementary strands, respectively.

## Conclusions

Magnetic bead capture has been shown to be a powerful tool for circumventing unwanted non-specific adsorption effects in label-free stripping-potentiometric DNA hybridization assays. In particular, the efficient magnetic separation has been



extremely useful for discriminating against unwanted constituents, including a large excess of mismatched and non-complementary oligomers, chromosomal DNA, RNA and proteins. Further improvements, particularly towards the detection of point mutations, are expected from combining the new protocol with peptide nucleic acid (PNA) probes. Such coupling of magnetic hybridization surfaces with renewable transducers and label-free electrical detection eliminates the needs for external indicators and advanced surface modification or regeneration schemes, and hence results in a greatly simplified protocol.

## Acknowledgements

J.W. acknowledges the financial support from the NIH (Grant No. R01 14549-02 and the Rise Program) and the US Army Medical Research (Award No. DAMD17-00-1-0366). A.K. and A.E. acknowledge fellowships from the Egyptian government and NATO [through the Turkish Scientific Research and Technical Council (TUBITAK)], respectively. A loan of the MCB 1200 Biomagnetic Processing Platform, provided by Dexter Co., is gratefully acknowledged.

## References

- 1 S. R. Mikkelsen, *Electroanalysis*, 1996, **8**, 15.
- 2 J. Wang, *Chem. Eur. J.*, 1999, **5**, 1681.
- 3 E. Palecek and M. Fojta, *Anal. Chem.*, 2001, **73**, 75A.
- 4 J. Wang, E. Palecek, P. Nielsen, G. Rivas, X. Cai, H. Shiraishi, N. Dontha, D. Luo and P. Farias, *J. Am. Chem. Soc.*, 1996, **118**, 7667.
- 5 S. Takenaka, K. Yamashita, M. Takagi, Y. Uto and H. Kondo, *Anal. Chem.*, 2000, **72**, 1334.
- 6 T. de Lumley, C. Campbell and A. Heller, *J. Am. Chem. Soc.*, 1996, **118**, 5504.
- 7 G. Marrazza, G. Chiti, M. Mascini and M. Anichini, *Clin. Chem.*, 2000, **46**, 31.
- 8 F. Patolsky, E. Katz, A. Bardea and I. Willner, *Langmuir*, 1999, **15**, 3703.
- 9 D. H. Johnston, K. Glasgow and H. H. Thorp, *J. Am. Chem. Soc.*, 1995, **117**, 8933.
- 10 C. Berggren, P. Stalhandske, J. Brundell and G. Johansson, *Electroanalysis*, 1999, **11**, 156.
- 11 E. K. Wilson, *Chem. Eng. News*, 1998, May, **25**, 47.
- 12 J. Wang, G. Rivas, J. Fernandes, J. L. Paz, M. Jiang and R. Waymire, *Anal. Chim. Acta*, 1998, **375**, 197.
- 13 A. Steel, T. Herne and M. Tarlov, *Anal. Chem.*, 1998, **70**, 4670.
- 14 *Advances in Biomagnetic Separations*, ed. M. Uhlin, E. Hornes and O. Olsvik, Eaton Publishing, Natick, 1994.
- 15 J. Wang, D. Xu, A. Erdem, R. Polsky and M. Salazar, *Talanta*, in press.
- 16 E. Palecek, S. Biirova, L. Havran, R. Kizek, A. Miaulkova and F. Jelen, *Talanta*, in press.
- 17 MCB1200 MixSep Technology, [http://www.sigris.com/mcb\\_technology.html](http://www.sigris.com/mcb_technology.html).
- 18 D. Tong, M. Stimpel, A. Reinthaller, N. Varva, S. Mullauer, S. Loedolter and R. Zeillinger, *Clin. Chem.*, 1999, **45**, 976.
- 19 J. Wang, A. Kawde and E. Sahlin, *Analyst*, 2000, **125**, 5.
- 20 J. Wang, A. N. Kawde, E. Sahlin, C. Parrado and G. Rivas, *Electroanalysis*, 2000, **12**, 917.
- 21 J. Wang, X. Cai, C. Jonsson and M. Balakrishnan, *Electroanalysis*, 1996, **8**, 20.

---

---

## **Silver-Enhanced Colloidal Gold Electrochemical Stripping Detection of DNA Hybridization**

---

**Joseph Wang, Ronen Polksky, and Danke Xu**

Department of Chemistry and Biochemistry, New Mexico State  
University, Las Cruces, New Mexico 88003

**Langmuir®**  
The ACS Journal of Surfaces and Colloids

Reprinted from  
Volume 17, Number 19, Pages 5739–5741

# Silver-Enhanced Colloidal Gold Electrochemical Stripping Detection of DNA Hybridization

Joseph Wang,\* Ronen Polksky, and Danke Xu

Department of Chemistry and Biochemistry, New Mexico State University,  
Las Cruces, New Mexico 88003

Received June 29, 2001

We report on a novel method for detecting DNA hybridization, based on the precipitation of silver on gold nanoparticle tags and a subsequent electrochemical stripping detection of the dissolved silver. Such coupling of a nanoparticle-promoted silver precipitation with the remarkable sensitivity of stripping metal analysis offers a dramatic enhancement of the hybridization response. An efficient magnetic isolation of the duplex is used for discriminating against nonhybridized DNA, including an excess of mismatched oligonucleotides. The new silver-enhanced colloidal gold stripping detection strategy holds great promise for the detection of DNA hybridization and represents an attractive alternative to indirect optical affinity assays of nucleic acids and other biomolecules.

## Introduction

Nanoparticle-based materials offer excellent prospects for chemical and biological sensing because of their unique optical and mechanical properties.<sup>1</sup> Silver deposition on gold nanoparticles is commonly used in histochemical microscopy to visualize DNA-conjugated gold particles. Mirkin and co-workers have developed DNA sensors using hybridization-induced changes in (distance-dependent) optical properties of gold-particle-modified oligonucleotides<sup>2</sup> and a scanometric DNA array based on silver amplification of a hybridization event.<sup>3</sup> Silver enhancement was also used for detecting single viral copies using *in situ* hybridization, providing an alternative for *in situ* polymerase chain reaction.<sup>4</sup> Inspired by such novel use of gold nanoparticle labeling and subsequent silver enhancement, the present communication aims at developing an analogous electrical route for gene detection. In particular, we wish to demonstrate the detection of DNA hybridization in connection to measurement of the deposited silver by the extremely sensitive technique of electrochemical stripping metal analysis.<sup>5</sup> While the new silver-enhanced colloidal gold stripping detection strategy is presented below in connection to DNA hybridization, it represents an attractive alternative to histochemical imaging of protein- and antibody-conjugated nanoparticles.

Figure 1 outlines the steps of the new particle-based bioelectronic protocol. A streptavidin-coated magnetic latex sphere (A) is bound to a biotinylated DNA probe (B). The hybridization event between the target nucleic acid and the captured probe (C) is followed by binding of streptavidin-coated 20 nm colloidal gold to the biotinylated target (D) and 10 min of catalytic silver precipitation onto the gold nanoparticles (E). The silver is then dissolved,

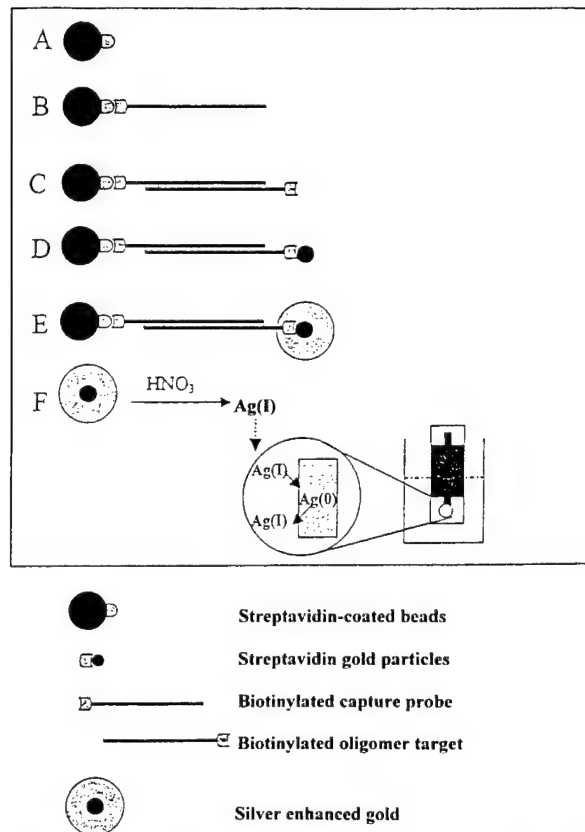


**Figure 1.** Schematic representation of the analytical procedure: (A) introduction of the streptavidin-coated beads; (B) addition and capture of the biotinylated probe; (C) addition of the biotinylated target and the hybridization event; (D) addition of the streptavidin–gold particles; (E) addition of the silver enhancer and formation of metallic silver tag; (F) dissolution of the silver tag and its stripping potentiometric detection.

\* Corresponding author. E-mail: joewang@nmsu.edu.

(1) (a) Templeton, A.; Wuelfing, W. P.; Murray, R. W. *Acc. Chem. Res.* **2000**, 33, 27. (b) Liu, J.; Alvarez, J.; Kaifer, A. *Adv. Mater.* **2000**, 12, 1381. (c) Dubertret, B.; Calame, M.; Libchaber, A. *J. Nat. Biotechnol.* **2001**, 19, 365.

(2) Storhoff, J. J.; Elghanian, R.; Mucic, R. C.; Mirkin, C. A.; Letsinger, R. L. *J. Am. Chem. Soc.*, **1998**, 120, 1959.

(3) Taton, T. A.; Mirkin, A. A.; Letsinger, R. L. *Science* **2000**, 289, 1757.

(4) Zehbe, I.; Hacker, G. W.; Su, H. C.; Hauser-Kronberger, C.; Hainfeld, J. F.; Tubbs, R. *Am. J. Pathol.* **1997**, 150, 1553.

(5) Wang, J. *Analytical Electrochemistry*, 2nd ed.; Wiley: New York, 2000.

and detected at a disposable thick-film carbon electrode (F) using a potentiometric stripping protocol.

## Results and Discussion

The new protocol couples the inherent signal amplifications of nanoparticle-promoted silver precipitation and of stripping metal analysis with effective discrimination

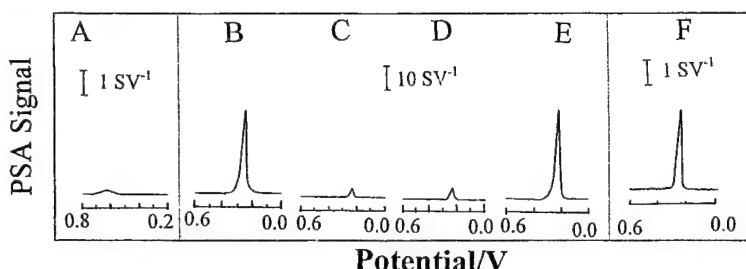


**Figure 2.** Chronopotentiometric stripping response for DNA detected by monitoring the gold nanoparticle tag (A) and the silver enhancer tag (B–F): 200 ng/mL target (A); 200 ng/mL target (B); 10  $\mu$ g/mL noncomplementary strand (C); 600 ng/mL three-base mismatched strand (D); a mixture of 200 ng/mL target and 10  $\mu$ g/mL noncomplementary strand (E); 20 ng/mL target (F). Gold assay conditions: (A) deposition, 1 min at  $-0.8$  V; stripping current,  $+3.0 \mu$ A. Silver assay conditions (B–F): deposition, 1 min at  $-0.5$  V; stripping current,  $+3.0 \mu$ A. Hybridization time, 20 min; amount of the magnetic beads (Bangs Laboratories), 50  $\mu$ g; amount of 20 nm streptavidin-coated gold particles (Energy Beam Science), 5  $\mu$ L. Silver Enhancer Solution (Sigma, equal volumes of solutions A and B), 30  $\mu$ L each; 60  $\mu$ L 2.5% sodium thiosulfate pentahydrate. Oligonucleotides (with 5' biotin modification) were acquired from Sigma-Genosys Ltd. and had the following sequences: biotin-5'GAT TTT CTT CCT TTT GTT C (immobilized probe, E908X-WT/P); biotin-5'GAA CAA AAG GAA AAT C (target, E908X-WT); biotin-5'GGT CAG GTG GGG GGT ACG CCA GG (noncomplementary strand, E908X); biotin-5' CAA CAA AAG CAA CAA AAT C (mismatched strand, E908X-WT/3bm). Chronopotentiometric measurements were performed with a TraceLab stripping unit PSU20 (Radiometer). DNA assays were carried out using the MCB 1200 Biomagnetic Processing Platform (Dexter Corp. Magnetic Technologies, Fremont, CA).

against nonhybridized DNA, the use of microliter sample volumes and single-use transducers, and hence offers great promise for decentralized genetic testing. Its attractive performance has been illustrated for the detection of DNA segments related to the BRCA1 breast cancer gene. Figure 2A shows the stripping response of the gold tag, from a sample containing 200 ng/mL (1.6 pmol) nucleic-acid target (using 1 M HBr/0.1 mM Br<sub>2</sub> as the dissolution and detection solutions),<sup>6</sup> while Figure 2B shows the corresponding silver hybridization stripping response after silver enhancement, dissolution, and deposition (in the “silver-enhancer solution”, a 50% HNO<sub>3</sub> medium, and 0.1 M HNO<sub>3</sub>/0.1 M KNO<sub>3</sub> electrolyte, respectively). The well-defined silver signal ( $E_p = 0.23$  V) is 125 times greater than that of the gold tag (1580 ms vs 12.5 ms; note the different scales). Substantially smaller signals are observed for a 50-fold excess (10  $\mu$ g/mL) of noncomplementary DNA and for a 3-fold excess of the three-base mismatched oligomer (parts C and D of Figure 1, respectively). Such minimization of nonspecific binding is attributed to the efficient magnetic separation, i.e., removal of nonhybridized DNA. The mixture response of Figure 2E also reflects the discrimination against an excess of unwanted constituents. Also shown (Figure 2F) is the response for a 5 ng/mL breast cancer DNA target, which indicates a low detection limit of around 0.2 ng/mL (32 pM). This corresponds to 10 pg (1.5 fmol) in the 50  $\mu$ L hybridization solution (in connection to a 20 min hybridization). Substantially lower detection limits are expected in connection to longer hybridization periods and/or deposition times. The electrochemical route offers well-defined concentration dependence. A calibration experiment over the 20–1000 ng/mL range resulted in a linear response (with a slope of 3.28 ms mL/ng). A series of eight repetitive measurements of the 400 ng/mL target solution was used for estimating the precision (20 min hybridization, not shown). This series yielded a mean peak area of 1550 ms and a relative standard deviation of 19%. Most favorable stripping detection of the dissolved silver tag was obtained using deposition at  $-0.5$  V and a stripping current of 3  $\mu$ A. The peak area increased linearly with the deposition time over the 0.5–10 min range, with 10 min deposition yielding ca. 83-fold enhancement of the response (vs that without accumulation).

(6) Dequaire, M.; Degrand, C.; Limoges, B. *Anal. Chem.* 2000, 72, 5521.

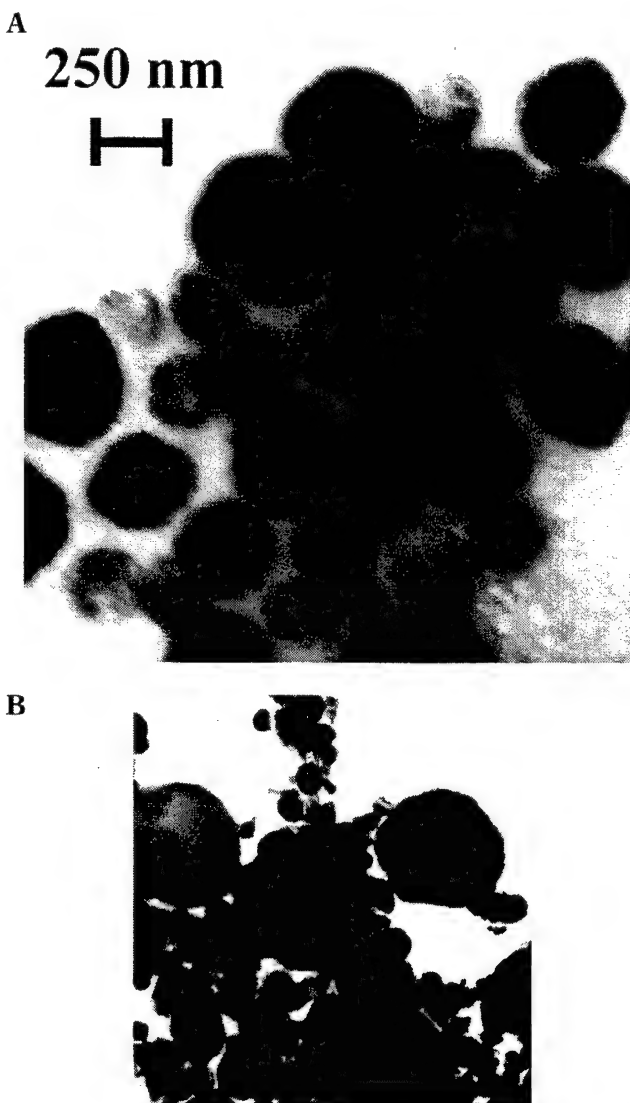


**Figure 3.** Transmission electron micrographs of a network structure resulting from the hybridization of a 50  $\mu$ g/mL target sample before (A) and after (B) the 8 min silver enhancement. Hybridization time was 20 min. Micrographs were taken with a Hitachi H7000 instrument, using an accelerating voltage of 75 kV.

The ultimate objective of the silver enhancement is to cause catalytic deposition of silver (on the gold tags), while avoiding spontaneous deposition onto other components of the system. Because analogous optical methods rely on a threshold amount of silver for visualization, excess silver ions are not of major concern. In contrast, an excess of silver can affect the reliability of the stripping-based electrical detection. It has been shown that the polyanionic DNA backbone itself can act as a nucleation site for silver growth through cation exchange with sodium and ion-pair complexation to the DNA bases.<sup>7</sup> Such adsorption of silver ions on the captured probe can lead to undesired background contributions. These "blank" signals can be eliminated by adding a sodium thiosulfate fixer solution (that transfers the silver cation into the  $\text{Ag}(\text{S}_2\text{O}_3)^5^-$  anion)<sup>8</sup> and by controlling the silver precipitation time. Precipitation periods shorter than 11 min assured that only the Au particle tags are coated with silver, with a 10 min period offering the best tradeoff between high sensitivity and selectivity.

Such initial silver nucleation onto the Au tags leads to a continuous deposition of silver on silver and eventually to coverage of the entire structure. A transmission electron micrograph before the silver enhancement (Figure 3A) shows a three-dimensional aggregate of the magnetic spheres (linked through the DNA hybrids and Au nanoparticles). In contrast, a nonuniform distribution of deposited silver, covering the entire aggregate, is observed following the silver enhancement (Figure 3B). Dissolution of this precipitate results in a high silver level, e.g., 13

(7) Braun, E.; Eichen, Y.; Sivan, U.; Ben-Yoseph G. *Nature* **1998**, *391*, 775.

(8) Henn, R. W. *Nebel's Handbook of Photography and Reprography Materials, Processes and Systems*; Litton Educational Publishing Inc.: 1977; p 114.

$\mu\text{g/mL}$ , as was indicated from comparison of the stripping response for a standard 100  $\text{ng/mL}$  silver solution and for the silver precipitated in connection to the hybridization of 5  $\text{ng/mL}$  DNA target (130 vs 17000 ms, respectively; conditions, as in Figure 2).

In conclusion, we described a novel electrochemical method for detecting DNA hybridization based on the precipitation of silver onto gold nanoparticle tags. The dramatic signal amplification advantage of the silver-enhanced colloidal gold stripping detection has been combined with an efficient magnetic removal of non-complementary DNA. The new method represents an attractive addition to the arsenal of electrochemical strategies for DNA analysis,<sup>9,10</sup> obviates the need for enzymes or fluorescence detection, and offers great promise for gene detection, in general. Analogous affinity assays of antibodies or proteins should also benefit from the attractive performance, simplicity, and portability of the new approach. The creation of DNA arrays, yielding multiple silver stripping peaks (in connection to microscopic wells and magnetic microelectrode transducers at the individual sites) can be envisioned. Direct stripping detection of the silver precipitate (contacting a magnetic electrode) without prior dissolution should also facilitate the creation and operation of such arrays. Preliminary results are very encouraging.

**Acknowledgment.** Financial support from the US Army Medical Research (Award No. DAMD17-00-1-0366) and the National Institutes of Health (Grant No. R01 14549-02) is gratefully acknowledged.

LA011002F

(9) Palecek, E.; Fojta, M. *Anal. Chem.* **2001**, *73*, 75A.

(10) Wang, J. *Chem. Eur. J.* **1999**, *5*, 1681.

---

# **Metal Nanoparticle-Based Electrochemical Stripping Potentiometric Detection of DNA Hybridization**

---

**Joseph Wang, Danke Xu, Abdel-Nasser Kawde, and Ronen Polksy**

Department of Chemistry and Biochemistry, New Mexico State  
University, Las Cruces, New Mexico 88003



Reprinted from  
Volume 73, Number 22, Pages 5576–5581

# Metal Nanoparticle-Based Electrochemical Stripping Potentiometric Detection of DNA Hybridization

Joseph Wang,\* Danke Xu, Abdel-Nasser Kawde, and Ronen Polksky

Department of Chemistry and Biochemistry, New Mexico State University, Las Cruces, New Mexico 88003

A new nanoparticle-based electrical detection of DNA hybridization, based on electrochemical stripping detection of the colloidal gold tag, is described. In this protocol, the hybridization of a target oligonucleotide to magnetic bead-linked oligonucleotide probes is followed by binding of the streptavidin-coated metal nanoparticles to the captured DNA, dissolution of the nanometer-sized gold tag, and potentiometric stripping measurements of the dissolved metal tag at single-use thick-film carbon electrodes. An advanced magnetic processing technique is used to isolate the DNA duplex and to provide low-volume mixing. The influence of relevant experimental variables, including the amounts of the gold nanoparticles and the magnetic beads, the duration of the hybridization and gold dissolution steps, and the parameters of the potentiometric stripping operation upon the hybridization signal, is examined and optimized. Transmission electron microscopy micrographs indicate that the hybridization event leads to the bridging of the gold nanoparticles to the magnetic beads. Further signal amplification, and lowering of the detection limits to the nanomolar and picomolar domains, are achieved by precipitating gold or silver, respectively, onto the colloidal gold label. The new electrochemical stripping metallogenomagnetic protocol couples the inherent signal amplification of stripping metal analysis with discrimination against nonhybridized DNA, the use of microliter sample volumes, and disposable transducers and, hence, offers great promise for decentralized genetic testing.

DNA hybridization biosensors hold an enormous potential for disease diagnosis, drug screening, or forensic applications.<sup>1</sup> Among these, electrochemical devices offer great promise for rapid, simple, and low-cost decentralized detection of specific nucleic acid sequences.<sup>2–4</sup> Various strategies have been developed for such electrical transduction of DNA hybridization. These include monitoring the increased electrochemical response of a redox-active indicator (that recognizes the DNA duplex)<sup>5,6</sup> and probing hybridization-induced changes in the intrinsic signal of nucleic acids<sup>7,8</sup> or of other interfacial properties.<sup>9,10</sup> The overall sensitivity of such electrical assays can be improved by using a label that

can be detected with high sensitivity. Oligonucleotide bearing enzyme labels (such as alkaline phosphatase or peroxidase)<sup>11,12</sup> or electroactive tags (such as ferrocene or anthraquinone)<sup>13,14</sup> have thus been used to generate highly sensitive electrical signals.

Here we report on a new nanoparticle-based electrochemical detection of DNA hybridization. Metal nanoparticles have attracted broad recent attention.<sup>15</sup> Such nanoparticles can bring novel capabilities to the sensing of DNA hybridization. Storhoff et al.<sup>16</sup> reported on a selective colorimetric detection of DNA sequences utilizing the distance-dependent optical properties of aggregated gold particles. Mirkin's group also reported on a scanometric DNA array detection based on nanoparticle-labeled oligonucleotide targets.<sup>17</sup> Oligonucleotide-functionalized metal nanoparticles were also used for microgravimetric transduction of the hybridization event in connection to a dendritic signal amplification.<sup>18</sup> Yet, electrochemical detection of DNA hybridization based on the use of metal nanoparticle tags has not been reported.

The present protocol uses a colloidal gold tag for electrochemical stripping detection and amplification of DNA hybridization. Stripping analysis is a powerful electroanalytical technique for trace metal measurements.<sup>19</sup> Its remarkable sensitivity is attributed to the “built-in” preconcentration step, during which the target metals are accumulated onto the working electrode. The detection limits are thus lowered by 3–4 orders of magnitude, compared to pulse-voltammetric techniques, commonly used for monitoring DNA hybridization. Highly sensitive electrochemical stripping analysis was used earlier for detecting metal ion tracers<sup>20,21</sup> or gold nanoparticle tags<sup>22</sup> in metal immunoassays but not in con-

- (1) Wang, J. *Nucleic Acids Res.* 2000, 28, 3011.
- (2) Mikkelsen, S. R. *Electroanalysis* 1996, 8, 15.
- (3) Palecek, E.; Fojta, M. *Anal. Chem.* 2001, 73, 74A.
- (4) Wilson, E. K. *Chem. Eng. News* 1998, (May 25), 47.
- (5) Millan, K.; Mikkelsen, S. R. *Anal. Chem.* 1993, 65, 2317.
- (6) Hashimoto, K.; Ito, K.; Ishimori, Y. *Anal. Chem.* 1994, 66, 3830.
- (7) Johnston, D. H.; Glasgow, K.; Thorp, H. H. *J. Am. Chem. Soc.* 1995, 117, 8933.
- (8) Wang, J.; Rivas, G.; Fernandes, J.; Paz, J. L.; Jiang, M.; Waymire, R. *Anal. Chim. Acta* 1998, 375, 197.
- (9) Berggren, C.; Stalhandske, P.; Brundell, J.; Johansson, G. *Electroanalysis* 1999, 11, 156.
- (10) Wang, J.; Jiang, M.; Fortes, A.; Mukherjee, B. *Anal. Chim. Acta* 1999, 402, 7.
- (11) de Lumley, T.; Campbell, C.; Heller, A. *J. Am. Chem. Soc.* 1996, 118, 5504.
- (12) Alfanta, L.; Singh, A. K.; Willner, I. *Anal. Chem.* 2001, 73, 91.
- (13) Ihara, T.; Nakayama, M.; Murata, M.; Nakano, K.; Maeda, M. *Chem. Commun.* 1997, 1609.
- (14) Kertez, V.; Whittermore, N. A.; Inamati, G.; Manoharan, M.; Cook, P.; Baker, D.; Chambers, J. Q. *Electroanalysis* 2000, 12, 889.
- (15) Schmid, G. *Clusters and Colloids. From Theory to Applications*; VCH: New York, 1994.
- (16) Storhoff, J. J.; Elghanian, R.; Mucic, R.; Mirkin, C. A.; Letsinger, R. L. *J. Am. Chem. Soc.* 1998, 120, 1959.
- (17) Taton, T. A.; Mirkin, C. A.; Letsinger, R. L. *Science* 2000, 289, 1757.
- (18) Patoolsky, F.; Ranjit, K. T.; Lichtenstein, A.; Willner, I. *Chem. Commun.* 2000, 1025.
- (19) Wang, J. *Stripping Analysis: Principles, Instrumentation, and Applications*; VCH Publishers: Deerfield Beach, FL, 1985.
- (20) Doyle, M. J.; Halsall, H. B.; Heineman, W. R. *Anal. Chem.* 1982, 54, 2318.
- (21) Wang, J.; Tian, B.; Rogers, K. R. *Anal. Chem.* 1998, 70, 1682.

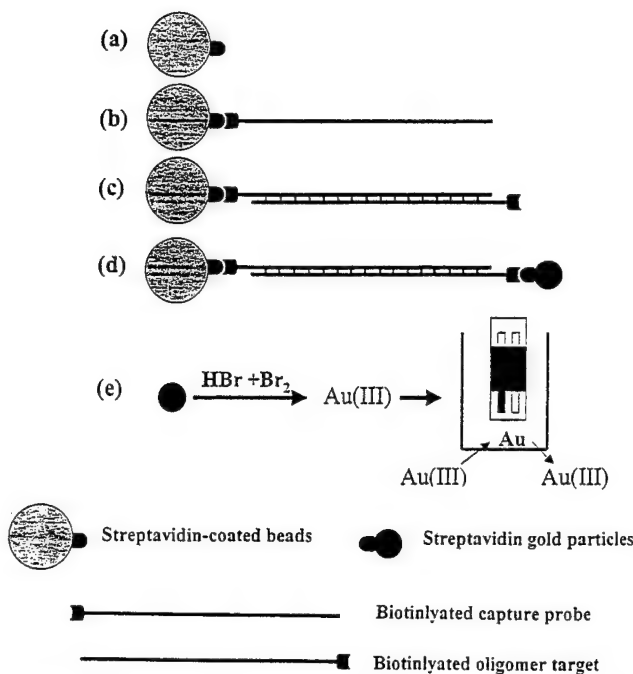


**Figure 1.** Schematic representation of the analytical protocol: (a) introduction of the streptavidin-coated beads; (b) immobilization of the biotinylated probe onto the magnetic beads; (c) addition of the biotinylated target—the hybridization event; (d) addition and capture of the streptavidin-gold nanoparticles; (e) dissolution of the gold tag and PSA detection.

nnection with the detection of DNA hybridization. The new nanoparticle-based electrochemical DNA detection has been combined with an advanced biomagnetic processing technology that couples an efficient magnetic removal of nonhybridized DNA with low-volume magnetic mixing.<sup>23</sup> The resulting protocol consists of the hybridization of a biotinylated target strand to oligonucleotide probe-coated magnetic beads, followed by binding of the streptavidin-coated gold nanoparticles to the captured target, and an acid dissolution and stripping-potentiometric detection of the gold tag at a disposable thick-film carbon electrode (Figure 1). The new electrochemical metallogenomagnetic assay thus combines the inherent signal amplification of stripping metal analysis with discrimination against nonhybridized DNA, the use of microliter sample volumes, and disposable transducers. Further enhancement of the indirect hybridization stripping signal is achieved by growing the gold nanoparticle tags into larger particles or by precipitating silver onto the gold. The optimization, characterization, and attractive performance characteristics of the nanoparticle-based electrochemical stripping detection of DNA hybridization are reported in the following sections in connection with the detection of nucleic acid segments related to the breast cancer BRCA1 gene.

## EXPERIMENTAL SECTION

**Apparatus.** Potentiometric stripping analysis (PSA) of the dissolved gold tag was performed with the TraceLab potentiometric stripping unit PSU20 (Radiometer). The preparation of the probe-coated magnetic beads and the hybridization reaction were performed on a MCB 1200 biomagnetic processing platform (Dexter Corp. Magnetic Technologies, Fremont, CA). Transmis-

sion electron micrographs (TEMs) were obtained with a Hitachi H7000 (using an accelerating voltage of 75 kV), by placing a 5- $\mu$ L droplet of the beads/nucleic acid/colloidal gold conjugate sample (in deionized water) onto a 3-mm-diameter, 200-mesh copper grid and allowing it to evaporate to dryness.

**Electrode Preparation.** The screen-printed electrodes (SPEs) were fabricated using a semiautomatic screen printer (model TF-100, MPM Inc., Franklin, MA). The carbon ink (Acheson 440B, Acheson Colloid Co., Ontario, CA) and the silver/silver chloride one (Ercon 414, Ercon, Wareham, MA) were printed onto alumina ceramic plates (33.5 mm  $\times$  101.5 mm, Coors Ceramic Co., Golden, CO) through a patterned stencil to give a group of 10 SPEs (each including a carbon working electrode and a Ag/AgCl reference electrode). The electrodes were cured for 1 h (at 150 °C) following each printing and were allowed to cool. A layer of insulator (ESL protective ink 240-5B, ESL Inc., King of Prussia, PA) was then printed onto a portion of the conducting “lines”, exposing a 2.0 mm  $\times$  6.0 mm working electrode area. The performance of the resulting electrode was evaluated by checking the background response. Electrodes displaying an abnormally high background were discarded.

**Materials and Reagents.** All stock solutions were prepared using deionized and autoclaved water. Tween 20 and MgSO<sub>4</sub> were purchased from Aldrich. Tris-HCl buffer, LiCl, Na<sub>2</sub>EDTA, NaCl, HBr, and bromine were obtained from Fisher; streptavidin-gold particles (5-nm diameter) and the 10-nm colloidal gold were received from Sigma. The gold enhancer solution (GoldEnhance) was received from Nanoprobe Inc. (Yaphank, NY). Proactive streptavidin-coated magnetic spheres (CMO1N-lot 4725) were purchased from Bangs Laboratories. Oligonucleotides (with 5'-biotin modification) were acquired from Sigma-Genosys Ltd. and had the following sequences:

immobilized probe, biotinylated E908X-WT(P):

biotin-5'GAT TTT CTT CCT TTT GTT C

target, biotinylated E908X-WT:

biotin-5'GAA CAA AAG GAA GAA AAT C

noncomplementary strand, biotinylated E908X:

biotin-5'GGT CAG GTG GGG GGT ACG CCA GG

mismatched strand, biotinylated E908X-WT (3 bm):

biotin-5' CAA CAA AAG CAA CAA AAT C

**Preparation of Oligomer-Coated Microspheres and Analytical Procedure.** The preparation of the bead/probe conjugates was carried out using a modified procedure recommended by Bangs Laboratories<sup>24</sup> using the MCB 1200 biomagnetic processing platform. Briefly, 90  $\mu$ g of streptavidin-coated microspheres (Figure 1a) was transferred into a 1.5-mL centrifuge tube. The microspheres were washed once with 100  $\mu$ L of TTL buffer (100 mM Tris-HCl, pH 8.0, 0.1% Tween 20, 1 M LiCl) and resuspended in 20  $\mu$ L of TTL buffer. Subsequently, 4  $\mu$ g of probe oligomer was added and incubated for 15 min at room temperature with gentle mixing. The immobilized probe (Figure 1b) was then separated

(22) Dequaire, M.; Degrand, C.; Limoges, B. *Anal. Chem.* 2000, 72, 5521.

(23) MCB1200-MixSep Technology. [http://www.sigris.com/mcb\\_technology.html](http://www.sigris.com/mcb_technology.html).

(24) Technote 101, Bangs Laboratories Inc., Fishers, IN.

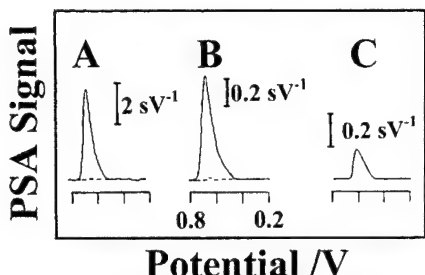


**Figure 2.** (A) Chronopotentiometric stripping response of  $5\ \mu\text{L}$  of  $10\text{-nm}$  colloidal gold particles ( $3.45 \times 10^8$  particles/mL). Gold oxidation time, 3 min; deposition time, 2 min at  $-0.8\ \text{V}$ . (B) Chronopotentiometric stripping response of  $100\ \text{ng/mL}$  Au(III), following 1-s (---) and 2-min (—) deposition. (C) Chronopotentiometric stripping analysis of  $4\ \text{ng/mL}$  Au(III); 2-min deposition at  $-0.8\ \text{V}$ . Stripping current,  $+5.0\ \mu\text{A}$ .

and washed sequentially with  $100\ \mu\text{L}$  of TT buffer (250 mM Tris-HCl, pH 8.0, 0.1% Tween 20),  $100\ \mu\text{L}$  of TTE buffer (250 mM Tris-HCl, pH 8.0, 0.1% Tween 20, 20 mM Na<sub>2</sub>EDTA, pH 8.0), and  $100\ \mu\text{L}$  of TT buffer and was resuspended in  $50\ \mu\text{L}$  of hybridization solution (750 mmol/L NaCl, 75 mmol/L sodium citrate). The desired amount of target was spiked, and the hybridization reaction was performed for a selected time (under magnetic stirring) at room temperature. The hybridized microsphere conjugates (Figure 1c) were then washed twice with TT buffer and resuspended in  $20\ \mu\text{L}$  of TTL buffer containing streptavidin–gold with gentle mixing for 15 min. The gold-labeled DNA conjugates (Figure 1d) were then washed twice with  $100\ \mu\text{L}$  of TT buffer, separated, and transferred into the gold oxidation and detection medium (1 mL of 1 M HBr containing 0.1 mM Br<sub>2</sub>). Several experiments involved an additional amplification step involving the catalytic precipitation of gold or silver onto the gold nanoparticle label.

**Chronopotentiometric Stripping Analysis.** Each experiment was carried out with a new electrode strip and included an initial background evaluation followed by the actual detection of the dissolved gold tag. PSA measurements were performed by cleaning the surface at  $+1.2\ \text{V}$  for 3 min followed by a 2-min deposition at  $-0.8\ \text{V}$  using a stirred 1.0 M HBr/0.1 mM Br<sub>2</sub> solution. Subsequent stripping was performed in a quiescent solution after a 5-s rest period using an applied anodic current of  $+5.0\ \mu\text{A}$ . The stripping curve data were filtered and baseline corrected with the TAP2 software.

## RESULTS AND DISCUSSION

The nanoparticle-based electrical bioassay consists of several steps, including the binding of the biotinylated probe to the streptavidin-coated magnetic beads, the actual DNA hybridization event, binding of the streptavidin-coated gold colloids to the captured biotinylated target, and the stripping-potentiometric detection of the dissolved gold tag at a disposable thick-film carbon electrode (Figure 1b–e, respectively). Detailed optimization of each of these steps, and characterization of the performance of the resulting protocol, are reported below.

**Optimization of Assay Conditions.** Figure 2A displays the response of the thick-film carbon sensor to  $3.45 \times 10^8$  10-nm gold nanoparticles (dissolved and measured in 1 M HBr/0.1 mM Br<sub>2</sub>) obtained using PSA. The computerized potentiometric stripping operation offers a sophisticated baseline fitting and data smoothing and, hence, results in a well-defined sharp gold peak ( $E_p = +0.68$

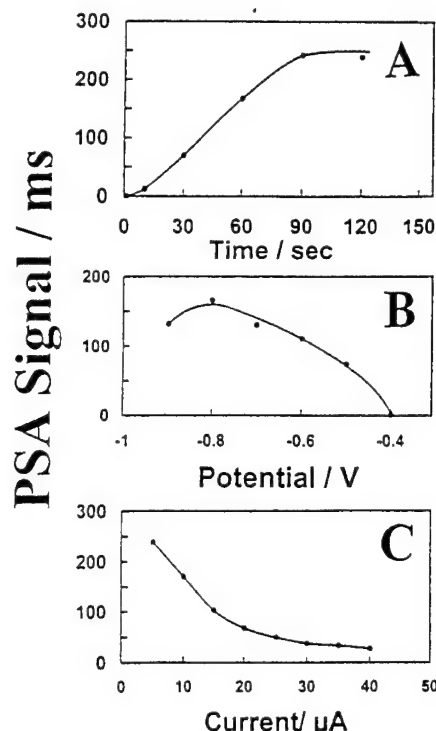


**Figure 3.** Optimization of the PSA protocol. Effect of the deposition time (A), deposition potential (B), and stripping current (C). (A) Deposition potential,  $-0.8\ \text{V}$ ; stripping current,  $+5.0\ \mu\text{A}$ ; (B) deposition time, 3 min; stripping current,  $+5.0\ \mu\text{A}$ ; (C) deposition for 2 min at  $-0.8\ \text{V}$ . Three-minute dissolution of  $10\ \mu\text{L}$  of  $10\text{-nm}$  colloidal gold particles containing  $6.9 \times 10^8$  particles/mL (in 1 mL of a 1 M HBr/0.1 mM Br<sub>2</sub> solution).

V) over a flat baseline (A). Such an attractive response indicates also that the use of disposable screen-printed electrodes does not compromise the attractive stripping performance of conventional (disk) electrodes. Also demonstrated in Figure 2 is the remarkable signal amplification associated with the deposition step of the electrochemical stripping operation (B). While a negligible response is observed for the  $100\ \text{ng/mL}$  (ppb) Au(III) solution following a 1-s deposition, the signal increases dramatically (>50-fold) following a 2-min deposition (dotted vs solid lines; Figure 2B). Such an effective preconcentration step permits convenient quantitation of trace (nanomolar) levels of gold. Figure 2C displays the PSA response for a  $4\ \text{ng/mL}$  ( $2 \times 10^{-8}\ \text{M}$ ) Au(III) solution following a 2-min deposition. The favorable signal-to-noise ratio (S/N) characteristics of these data indicate a detection limit of  $\sim 4 \times 10^{-9}\ \text{M}$  ( $0.7\ \text{ng/mL}$ ; S/N = 3). A similar detection limit ( $5 \times 10^{-9}\ \text{M}$ ) was reported for analogous voltammetric stripping measurements.<sup>22</sup> Further signal amplification and lowering of the detection limits are expected in connection to longer deposition times.<sup>19</sup>

The effect of the deposition time upon the gold PSA signal is further examined in Figure 3A. The peak area increases in a nearly linear fashion up to 90 s and then levels off. Other parameters of the PSA operation were optimized (Figure 3). The dependence of the stripping signal on the deposition potential was examined over the  $-0.4$  to  $-0.9\ \text{V}$  range (B). The response rises gradually between  $-0.4$  and  $-0.8\ \text{V}$  and then decreases slowly. The gold peak decreases linearly upon increasing the stripping current between  $5$  and  $15\ \mu\text{A}$ , then more slowly, and nearly levels off above  $30\ \mu\text{A}$  (C). All subsequent work thus employed a 2-min deposition at  $-0.8\ \text{V}$  in connection with a stripping current of  $5\ \mu\text{A}$ .

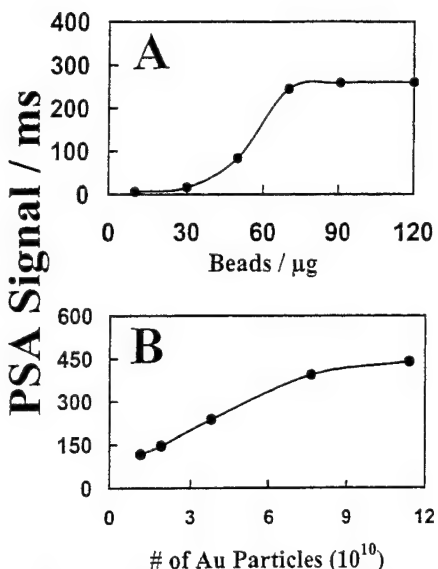


**Figure 4.** Effect of the amount of magnetic beads (A) and amount of streptavidin-coated gold particles (B) upon the hybridization response to the  $20 \mu\text{g/mL}$  target. Probe concentration,  $200 \mu\text{g/mL}$ ; amount of the 5-nm streptavidin-coated gold particles (A),  $3.8 \times 10^{10}$ ; amount of the magnetic beads (B),  $90 \mu\text{g}$ ; probe concentration,  $200 \mu\text{g/mL}$ ; hybridization time, 20 min. Other conditions, as in Figure 2.

The amounts of the magnetic beads and of the gold nanoparticles affect the quantity of bound probes and captured tags, respectively, and hence have a profound effect upon the sensitivity (Figure 4). The hybridization gold signal increases slowly by raising the amount of magnetic beads between 10 and  $30 \mu\text{g}$ , then more rapidly, and reaches a constant value above  $70 \mu\text{g}$  (A). Subsequent work employed  $90 \mu\text{g}$  of beads, which corresponded to  $1.71 \mu\text{g}$  of captured probe (based on the  $19 \mu\text{g}$  of biotinylated probe/mg of binding capacity of the spheres).<sup>24</sup> An excess amount of the probe,  $4 \mu\text{g}$ , was employed to ensure a full surface coverage. The stripping response increases nearly linearly upon raising the number of gold nanoparticles between  $1.1 \times 10^{10}$  and  $7.6 \times 10^{10}$  and then more slowly (B). All further work employed  $7.6 \times 10^{10}$  metal particle tags.

The TEM micrographs of Figure 5 indicate that the hybridization event links the gold nanoparticles to the magnetic beads. Figure 5A shows a large ( $7.6 \mu\text{m}$ ) magnetic bead, with a cluster of smaller ( $0.8\text{--}2.5 \mu\text{m}$ ) ones in its center, resulting from the DNA hybridization. (The distorted appearance of the large bead is due to melting from the high intensity of the electron beam.) A magnified portion of the outer edge (Figure 5B) clearly shows the 5-nm gold particles (as black dots; indicated by the arrows). The presence of gold was confirmed by its electron diffraction pattern; no such gold pattern was observed by replacing the target DNA with a noncomplementary one. Repeated washing of the samples (along with the magnetic separation), before placement on the grid, eliminated nonspecific gold signals in connection with noncomplementary oligomers. The appearance of gold particles (in Figure 5) can only be the result of conjugation with DNA hybrid. Such TEM observations are clearly supported by the electrochemical data (reported below). Recent nanoparticle aggregation models using reactive ligands and multifunctional receptors predict a distinct transition between limited and com-

plete aggregation as a function of the ligand-to-receptor ratio.<sup>25,26</sup> The cluster of beads of Figure 5C also shows gold particles (indicated by arrows) on the outer edge of the beads. Such particles appear to "bridge" the magnetic beads (in connection with the DNA hybrids that are not visible). The concave shape of the gold particles on the outer edge suggests that they are due to other "overlapping" beads (out of the plane of Figure 5C). The significantly higher degree of aggregation observed in the presence of complementary strands, as compared to noncomplementary ones (not shown), supports the possibility of linking between the beads through multiple streptavidin sites on the gold particles (which is consistent with nanoparticle aggregation models).<sup>25,26</sup> The implications of such assemblies upon the analytical performance are discussed below.

The duration of the new assay and its sensitivity are strongly influenced by the hybridization time and the gold dissolution period. Figure 6A displays the effect of the hybridization time upon the stripping hybridization signal. The response increases linearly with the hybridization time up to 10 min, then more slowly, and levels off above 20 min. The influence of the gold oxidation time is shown in Figure 6B. The response increases slowly between 0 and 2 min, then more rapidly, and levels off above 5 min. Apparently, such a period is sufficient for a complete dissolution of the gold tag. A similar period was employed in analogous metalloimmunoassays.<sup>22</sup> Note that the gold dissolution continues during the 2-min PSA deposition step; this accounts for the response observed at 0-min dissolution.

**Analytical Performance.** The attractive performance of the new electrochemical metallogenomagnetic assay has been illustrated for the detection of DNA segments related to the breast cancer BRCA1 gene.<sup>27</sup> The efficient magnetic isolation of the hybrid is particularly attractive for an electrical detection of DNA hybridization which is commonly affected by the presence of nonhybridized nucleic acid adsorbates. The specificity of the new nanoparticle genomagnetic assay is examined in Figure 7. A well-defined gold stripping response is observed for the  $25 \mu\text{g/mL}$  target solution following a 20-min hybridization (B). In contrast, a negligible PSA signal is observed for a 5-fold higher ( $100 \mu\text{g/mL}$ ) level of a noncomplementary oligomer (C). Note that such effective discrimination is observed at the bare electrode strip (without any "blocking" layer), reflecting the efficient magnetic removal of nonhybridized oligonucleotides and, hence, the absence of nonspecific binding. A three-base mismatch strand solution (at  $40 \mu\text{g/mL}$ ) yielded a response that is significantly ( $>65\%$ ) smaller than that of the  $25 \mu\text{g/mL}$  breast cancer target (D vs B). While such partial hybridization is not addressed by the magnetic isolation, the contribution of an excess mismatched oligonucleotide is not significant (and may be further minimized using PNA probes or thermal control). No response is observed for the blank ("zero target") solution (A). The mixture analysis (of Figure 7E,b) further demonstrates the efficient removal of noncomplementary nucleic acid adsorbates and the resulting minimization of nonspecific binding effects. An addition of a 4-fold excess of the noncomplementary strand has a negligible effect upon the response for the  $25 \mu\text{g/mL}$  target (Figure 7E; a vs b).

(25) Kissak, E. T.; Kennedy, M. T.; Trommeshauser, D.; Zasadzinski, J. A. *Langmuir* 2000, 16, 2825.

(26) Connolly, S.; Cobbe, S.; Fitzmaurice, D. *J. Phys. Chem. B* 2001, 105, 2222.

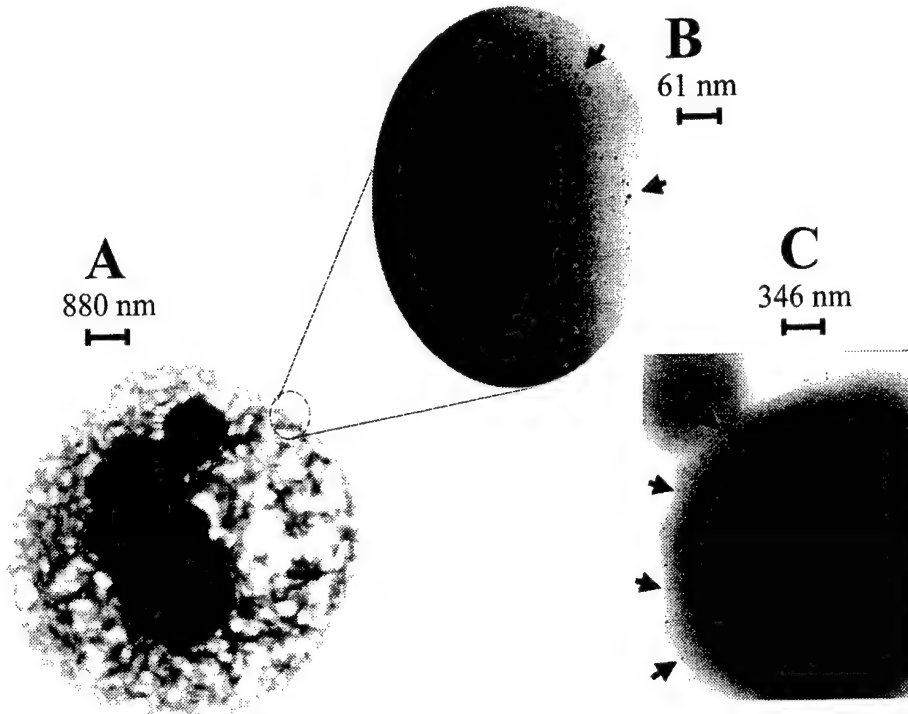


**Figure 5.** TEM of a network structure resulting from the hybridization of a 50  $\mu\text{g}/\text{mL}$  target sample at (A) 20K, (B) 60K and (C) 57K magnifications. Arrows indicate the 5-nm colloidal gold particles.

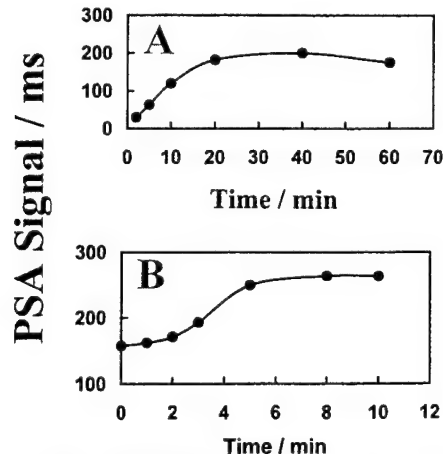


**Figure 6.** Effect of hybridization time (A) and gold oxidation time (B). Target concentration, 20  $\mu\text{g}/\text{mL}$ ; gold oxidation time (A), 3 min; hybridization time (B), 20 min; amount of magnetic beads, 70  $\mu\text{g}$ ; amount of the 5-nm streptavidin-coated gold particles,  $3.8 \times 10^{10}$ . Other conditions, as in Figure 2.

Figure 8 displays the dependence of the PSA response upon the concentration of the breast cancer DNA target. The peak area increases rapidly with the target concentration at first (up to 5  $\mu\text{g}/\text{mL}$ ), then more slowly, and starts to level off above 20  $\mu\text{g}/\text{mL}$  (A). Such curvature reflects not only the saturation of the probe hybridization sites but also the particle aggregation (illustrated in Figure 5), i.e., to the fact that a given metal tag can share multiple DNA hybrids. Such curvature can be addressed by using shorter hybridization times or in connection with a logarithmic scale. The latter results in a highly linear response up to 20  $\mu\text{g}/\text{mL}$ , with a leveling off thereafter (Figure 8B). A similar logarithmic scale was employed in analogous metalloimmunoassays.<sup>22</sup> Also shown in Figure 8A is the actual chronopotentiometric signal of the first point of these calibration data,

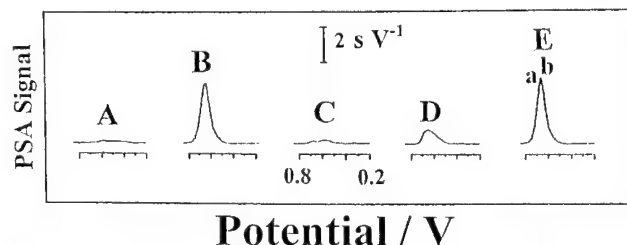


**Figure 7.** PSA hybridization response to 0  $\mu\text{g}/\text{mL}$  target (A); 25  $\mu\text{g}/\text{mL}$  target (B and E,a); 100  $\mu\text{g}/\text{mL}$  noncomplementary strand (C); 40  $\mu\text{g}/\text{mL}$  three-base mismatched strand (D); a mixture of 25  $\mu\text{g}/\text{mL}$  target and 100  $\mu\text{g}/\text{mL}$  noncomplementary strands (E,b). Hybridization time, 20 min; amount of magnetic beads, 90  $\mu\text{g}$ ; amount of 5-nm streptavidin-coated gold particles,  $7.6 \times 10^{10}$ . Other conditions, as in Figure 2.

corresponding to the 1.0  $\mu\text{g}/\text{mL}$  target concentration. Such response ( $0.3 \text{ s } \text{V}^{-1}$ ), along with the corresponding noise level ( $0.01 \text{ s } \text{V}^{-1}$ ), indicates a detection limit of 100  $\text{ng}/\text{mL}$  (i.e., 15 nM)-in connection with the 2-min short hybridization time (based on  $S/N = 3$ ). Such a detection limit corresponds to 5 ng in the 50- $\mu\text{L}$  samples. Further lowering of the detection limit is expected in connection with longer hybridization time or deposition periods, larger gold particles, or subsequent metal precipitation (described below). A series of eight repetitive measurements of the 20  $\mu\text{g}/\text{mL}$  target solution was used to estimate the precision (20-min hybridization; not shown). This series yielded a mean peak area of 228 ms and a relative standard deviation of 12%.

Further amplification of the sensitivity of the present nanoparticle-based stripping potentiometric DNA detection protocol can be achieved by catalytic precipitation of gold, known to produce larger particles.<sup>28</sup> Figure 9 compares the PSA hybridization response in the absence (A) and presence (B) of the nanoparticle-

(27) Tong, D.; Stimpel, M.; Reinhaller, A.; Varva, N.; Mullauer, S.; Loedolter, S.; Zeillinger, R. *Clin. Chem.* 1999, 45, 976.

(28) Brown, K. R.; Natan, M. J. *Langmuir* 1998, 15, 3703.

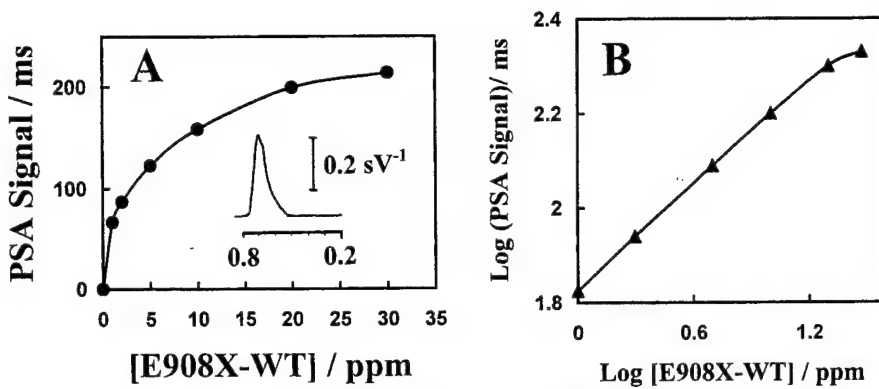


**Figure 8.** Calibration plot (A) and log–log calibration data (B) for the breast cancer E908X-WT target. Hybridization time, 2 min; amount of magnetic beads 90  $\mu\text{g}$ ; amount of 5-nm streptavidin-coated gold particles,  $7.60 \times 10^{10}$ ; gold oxidation time, 5 min. Also shown is the PSA hybridization signal of 1  $\mu\text{g}/\text{mL}$  target (A). Other conditions, as in Figure 2.

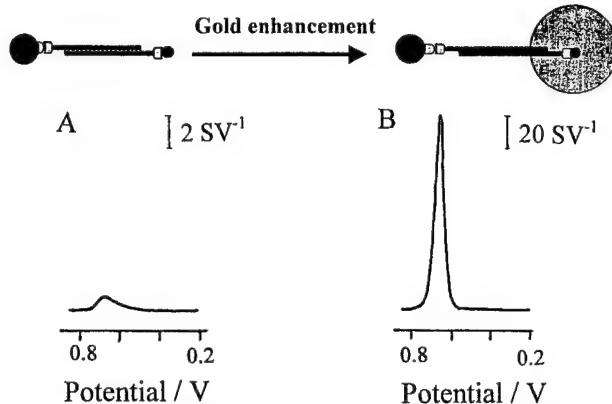


**Figure 9.** Effect of the gold enhancement upon the stripping response for the 10  $\mu\text{g}/\text{mL}$  E908X-WT target. (A) Stripping signal of the colloidal gold label; (B) same as (A) but after 10 min in the gold enhancing solution. Hybridization time, 25 min; amount of magnetic beads 90  $\mu\text{g}$ ; amount of 5-nm streptavidin-coated gold particles,  $7.60 \times 10^{10}$ ; gold oxidation time, 5 min. Other conditions, as in Figure 2.

seeded gold precipitation step. A dramatic (>80-fold) enhancement of the gold stripping signal is observed in connection with a 10-min gold precipitation reaction (Figure 9A vs B; note the different scales). While offering very favorable signal-to-noise characteristics, such an amplification route leads also to an increase in the background response (due to nonspecific binding of the gold ions with the magnetic beads and the oligonucleotide probe). Such background contribution limits the detectability to the 10 ng/mL (1.5 nM) target level (not shown), which represents only a 10-fold lowering of the detection limit. The minimization of the gold background signal is currently under investigation. A similar catalytic precipitation of silver (on the gold) offered picomolar detection limits (not shown). The coupling of the gold nanoparticle tags with additional amplification units (e.g., “treelike” dendrimers) and pathways should push the detection limits to the femtomolar domain. Analogous nanoparticle-based optical DNA measurements resulted in detection limits of 0.1 nM and 1 pM, in connection “scanometric”<sup>17</sup> or light-scattering<sup>29</sup> detection schemes, respectively.

In conclusion, we have demonstrated for the first time the use of electrochemical stripping metal analysis for monitoring DNA hybridization. The new electrochemical stripping metallogenomagnetic protocol combines the inherent signal amplification of

stripping metal analysis with effective discrimination against nonhybridized DNA (and other nonspecific adsorbates), the use of microliter sample volumes, and disposable transducers and, hence, offers great promise for centralized and decentralized genetic testing. Hand-held, battery-operated PSA instruments, developed for on-site detection of trace metals,<sup>30</sup> could facilitate such decentralized DNA diagnostic applications. The coupling of PNA probes with the metal–nanoparticle electrochemical detection route should lead to an effective amplification of mismatch-recognition events. Additional improvements in the detection limits are anticipated by coupling the electrochemical stripping detection with other amplification pathways (e.g., dendritic structures bearing multiple metal particles). While particle-labeled targets have been widely used for optical DNA detection,<sup>17</sup> the need for labeling the target can be obviated by using a second labeled probe in a sandwich assay format (i.e., a three-component assembly). One can also envision the use of different metal tags that may open the door to the simultaneous detection of multiple targets, in a manner analogous to the optical detection of Mirkin.<sup>29</sup> Current work in our laboratory aims at developing microfluidic devices, integrating and automating the various steps of the new electrochemical stripping metallogenomagnetic protocol. Such coupling of gold nanoparticles, electrochemical stripping analysis of the dissolved gold tags, and magnetic isolation of the hybrid on single microchip platforms can bring new capabilities to the detection of DNA hybridization.

#### ACKNOWLEDGMENT

This work was supported by the National Institutes of Health (Grant R01 14549-02) and U.S. Army Medical Research (Award DAMD17-00-1-0366). A loan of the MCB1200 Biomagnetic Processing Platform, provided by Dexter Co., is gratefully acknowledged. A.-N.K. acknowledges a fellowship from the Egyptian government.

Received for review June 26, 2001. Accepted September 11, 2001.

AC0107148

(30) Yarnitzky C.; Wang, J.; Tian, B. T. *Talanta* 2000, 51, 333.

# Magnetic-field stimulated DNA oxidation

Joseph Wang \*, Abdel-Nasser Kawde

Department of Chemistry and Biochemistry, New Mexico State University, P.O. Box 30001, Las Cruces, NM 88003-8001, USA

Received 12 February 2002; received in revised form 19 February 2002; accepted 19 February 2002

---

## Abstract

A reversible and cyclic magnetic-field stimulated DNA oxidation is described. Positioning an external magnet below the electrode attracts the DNA-functionalized magnetic particles to the surface, and stimulates the oxidation of the guanine nucleobases. Using a dual carbon-paste electrode assembly we demonstrate a spatially controlled DNA oxidation, with an 'ON/OFF' switching of the electron-transfer reaction upon relocating the external magnetic field. The process can be reversed and repeated upon switching the position of the magnet, with and without oxidation signals in the presence and absence of the magnetic field, respectively. We also demonstrate a 'magnetic' carbon-paste electrode, with an internal magnet, that collects the DNA-modified beads and stimulates the DNA oxidation process. The site-specific activation of the DNA oxidation holds promise for new DNA arrays and other geno-electronic applications. © 2002 Elsevier Science B.V. All rights reserved.

**Keywords:** Magnet; DNA; Carbon-paste electrode; Guanine oxidation

---

## 1. Introduction

The electrochemical activity of nucleic acids was discovered about four decades ago [1]. In particular, the electroreduction of nucleic acid bases has led to the development of pulse-polarographic [2] and adsorptive-stripping voltammetric [3] protocols for detecting trace levels of DNA and RNA at mercury drop electrodes. We have demonstrated that analogous trace measurements of nucleic acids can be performed by coupling their adsorptive accumulation onto carbon-paste electrodes with chronopotentiometric measurements of the guanine moiety [4,5]. Such electrochemical protocols offer great promise for the development of DNA hybridization biosensors and chips, for the detection of DNA damage, or for elucidating the interactions of nucleic acids with various drugs [6].

Here we wish to report on the reversible magnetic-field stimulated DNA oxidation. The ability of external magnetic fields to control electrochemical processes, such as biocatalytic transformations of redox enzymes [7] and the electrical generation of light [8], was recently

documented. Magnetic fields have also proven valuable for removing unwanted constituents in nucleic-acid assays [9,10], but not for triggering the electron-transfer reactions of DNA. In the following sections we will illustrate a site-specific DNA oxidation in connection with a dual carbon-paste electrode assembly (Fig. 1). Changing the position of the magnet (below these electrodes) is used for 'ON/OFF' switching of the DNA electron-transfer reaction (through attraction and removal of DNA functionalized-magnetic particles). We also demonstrate a magnetic carbon-paste electrode, with a built-in magnetic field.

## 2. Experimental

### 2.1. Apparatus

Chronopotentiometric measurements were performed with a potentiometric stripping unit PSU20 (Radiometer), controlled by a PC using the TAP2 software (Radiometer). The preparation of the oligomer-coated microspheres was performed on an MCB 1200 Bi-magnetic Processing Platform (Dexter Corporation Magnetic Technologies, Fremont, CA, USA). The planar dual-carbon paste electrode was fabricated by

\* Corresponding author. Tel.: +1-505-646-2140; fax: +1-505-646-6033.

E-mail address: [joewang@nmsu.edu](mailto:joewang@nmsu.edu) (J. Wang).

preparing two identical rectangular cavities ( $5.5 \times 4.0 \text{ mm}^2$  area; 3.0 mm depth), with a 3.0 mm spacing, on a plastic strip ( $20 \times 50 \times 4 \text{ mm}^3$ ). Copper wires, embedded into the plastic strip, provided the electrical contact. An open plastic tube (16 mm diameter, 7 mm long) provided the ‘wall’ of the electrochemical cell. The reference electrode (Ag/AgCl, Model MW2021, BAS, W. Lafayette, IN, USA) and the platinum wire counterelectrode were inserted into the resulting 1 ml cell through openings in its Teflon cover.

The integrated magneto-carbon paste sensor was prepared by placing a small magnet (2.0 mm-diameter, 1.0 mm height) in the cavity of a conventional carbon paste disk electrode (diameter, 2.6 mm; depth, 2 mm; Model CH104, CH Instruments). The Ag/AgCl reference and platinum-wire counter electrodes were inserted into the conventional 1 ml (‘beaker-like’) cell through holes in its Teflon cover.

## 2.2. Reagents

All stock solutions were prepared using deionized and autoclaved water. Sodium acetate buffer (3 M, pH 5.2 at 25 °C), Tris-HCl buffer, LiCl and NaCl were purchased from Sigma. Tween 20 was purchased from Aldrich. Proactive streptavidin-coated microspheres (CMO1N-lot 5205) were purchased from Bangs Laboratories.

The DNA oligonucleotides (with 5'-biotin modification) were obtained from Life Technologies (Grand Island, NY, USA), and had the following sequences:

- *Biotinylated Oligomer I:* biotin-5'GGC CGA CTC ACT GCG CGT CTT CTG TCC CGC CTT TTT CG
- *Biotinylated Oligomer II:* biotin-5'GAT TTT CTT CCT TTT GTT C

## 2.3. Electrode preparation

Carbon-paste electrodes (CPEs) were prepared by hand-mixing 70 mg of graphite powder and 30 mg mineral oil. A portion of the resulting paste was then packed firmly into the electrode cavities to yield rectangular-shaped dual-electrodes each with an active surface area of  $22.0 \text{ mm}^2$ . The resulting paste surfaces were smoothed (with a weigh paper) and rinsed carefully with double-distilled water prior to measurements. The integrated magnetic electrode was prepared in a similar fashion but in connection to an electrode cavity containing the magnet.

## 2.4. Preparation of the oligomer-coated microspheres

The bead preparation was carried out on the MCB 1200 Biomagnetic Processing Platform [11], using a modified procedure recommended by Bangs Laboratories (Technical Note 101). Hundred  $\mu\text{g}$  of the streptavidin-coated microspheres were transferred into a 1.5 ml

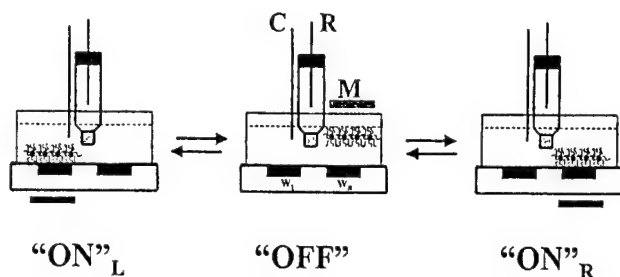


Fig. 1. Magneto-triggered spatially controlled DNA oxidation. The electrochemical cell contains the dual-carbon paste electrode ( $W_L$  and  $W_R$ ), the platinum wire counterelectrode (C), the Ag/AgCl reference electrode (R), and 1 ml acetate buffer solution (0.2 M, pH 5) containing the DNA-functionalized magnetic beads. The DNA oxidation is induced (“ON”) by placing the magnet (M) under the corresponding working electrode. Subsequent movements of the magnet, M, result in removal of the DNA-bound particles from the surface to the bulk solution (“OFF”), and their collection onto the second working electrode.

centrifuge tube. The microspheres were washed with 90  $\mu\text{l}$  TTL buffer (100 mM Tris-HCl, pH 8.0, and 0.1% Tween 20 and 1 M LiCl) and resuspended in 21  $\mu\text{l}$  TTL buffer. Subsequently, 10  $\mu\text{g}$  of the biotinylated oligonucleotide (in 4  $\mu\text{l}$  autoclaved water) were added and incubated for 20 min at room temperature with gentle mixing. The DNA-functionalized particles were then separated, washed twice with 90  $\mu\text{l}$  acetate buffer solution (0.2 M, pH 5), and resuspended into a 50  $\mu\text{l}$  acetate buffer solution.

## 2.5. Procedure

The electrochemical cell was filled with 950  $\mu\text{l}$  acetate buffer supporting electrolyte solution. Both electrodes were pre-treated by applying a potential of +1.7 V for 10 s, before introducing the DNA-bound beads to the detection cell. The electrochemical detection was stimulated by positioning the magnet (M) below the corresponding working electrode ( $W_L$ ) for attracting the functionalized magnetic particles (Fig. 1, “ON<sub>L</sub>”), and applying a constant anodic current of +5  $\mu\text{A}$ . The removal of the DNA-bound magnetic beads from the  $W_L$  surface was accomplished by placing the magnet on the cover of the electrochemical cell for 3 min, and collecting the modified particles at the solution surface (Fig. 1, “OFF”). Replacing the magnet under the second ‘right-side’ working electrode ( $W_R$ ) led to collection of the functionalized magnetic beads on its surface (Fig. 1, “ON<sub>R</sub>”), followed by anodic (chronopotentiometric) detection of the bound nucleic acid. The process was repeated for additional cycles.

## 3. Results and discussion

The dual carbon-paste electrode assembly has been used for demonstrating the spatially controlled DNA

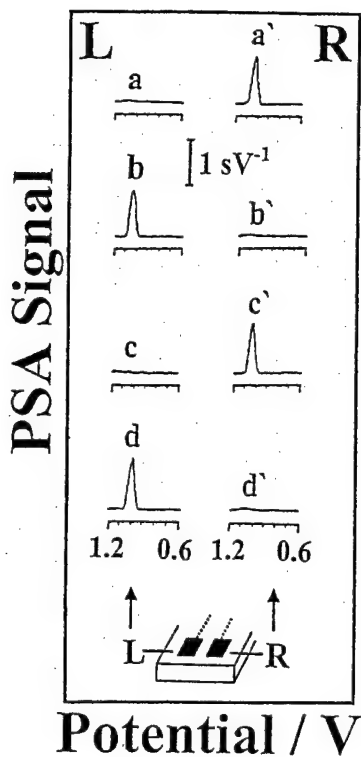


Fig. 2. Chronopotentiometric signals for the DNA oligomer I using the dual-carbon paste electrode assembly. a, b, c, and d are potentiograms obtained at the 'left' (L) electrode, while a', b', c', and d' are potentiograms obtained at the 'right' (R) electrode. a, b', c, and d' are potentiograms obtained in the absence of the magnet, while a', b', c', and d are potentiograms recorded in the presence of the magnet. Amount of magnetic beads, 100 µg; oligomer I DNA; beads collection time, 3 min. Pre-treatment potential, +1.7 V for 10 s; stripping current, +5 µA (between 0.6 and 1.2 V).

oxidation. Fig. 2 displays chronopotentiograms obtained at the 'left' (L) and 'right' (R) electrodes in the presence of the DNA-functionalized magnetic-beads upon placing the magnet alternately below these electrodes (cycles a-d). A well-defined response, corresponding to the oxidation of the guanine moiety ( $E_p = 1.02$  V), is observed upon placing the magnet below the 'right' electrode (a'). Apparently, the magnetic collection facilitates the contact of the guanine nucleobase with the surface, and hence the electron-transfer reaction. In contrast, no oxidation signal is observed at the 'left' electrode in the absence of an external magnetic field (a). The DNA oxidation at the 'right' electrode is switched 'off' by lifting the DNA-modified magnetic particles upward, i.e., removing them from the surface (Fig. 1, center). Switching the position of the magnet to the 'left' electrode results in a defined response (b) and no signal at the 'right' one (b'). The process can be reversed and repeated upon changing the position of the magnet (from the left to right electrodes), with and without oxidation signals in the presence and absence of the magnetic field, respectively (steps c and d).

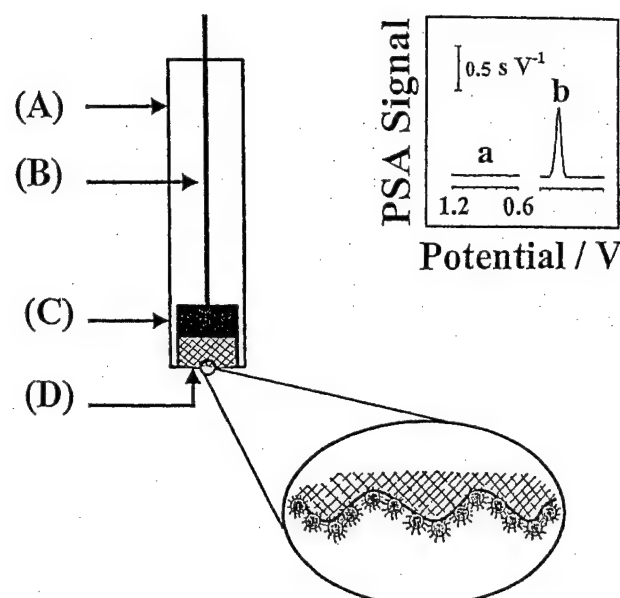


Fig. 3. Schematic representation of the integrated magneto-carbon paste electrode (MCPE): (A) the Teflon support; (B) copper wire contact; (C) internal magnet; (D) electrode cavity tightly packed with the carbon paste, along with the collected beads at the electrode surface. The inset displays the chronopotentiometric stripping signals of the DNA (oligomer II)-modified magnetic beads (50 µg) in the absence (a) and presence (b) of the magnet.

Instead of placing the magnet under the electrode it is possible to integrate it within the cavity of the carbon-paste transducer. Such a magnetic carbon-paste electrode, with a built-in magnetic field is illustrated in Fig. 3. The magnetic field (created by the internal magnet) can thus be used for collecting the bead-captured DNA and triggering the DNA oxidation. For example, the inset of Fig. 3 displays chronopotentiograms for the oligonucleotide-functionalized beads using the conventional (a) and magnetic (b) carbon-paste electrodes. No response is observed at the conventional electrode, as expected from the absence of (magnetic or adsorptive) accumulation. In contrast, the magnetic electrode displays a well-defined oxidation peak, reflecting the effective magnetic attraction.

#### 4. Conclusions

We have demonstrated a reversible and cyclic magnetic-field stimulated DNA oxidation. Changing the position of the magnet (at the dual electrode assembly) was shown useful for 'ON/OFF' switching of the DNA electron-transfer reaction. Such magnetic triggering of the DNA oxidation holds great promise for DNA arrays (based on closely spaced electrodes and guanine-free inosine-substituted probes), for stimulating charge-transfer through DNA, and for other genoelectronic applications. Such laterally activated DNA arrays are currently being designed in our laboratory.

### Acknowledgements

This research was supported by grants from NIH (Grant No. R01 14549-02) and the US Army Medical Research (Award No. DAMD17-00-1-0366). A fellowship from the Egyptian government (to AK) is acknowledged.

### References

- [1] E. Palecek, *Nature* 188 (1960) 656.
- [2] M. Vojtiskova, E. Lukasova, E. Palecek, *Bioelectrochem. Bioenerg.* 8 (1981) 487.
- [3] E. Palecek, M. Fojta, *Anal. Chem.* 66 (1994) 1566.
- [4] J. Wang, X. Cai, C. Johnson, M. Balakrishnan, *Electroanalysis* 8 (1996) 20.
- [5] J. Wang, X. Cai, J. Wang, C. Johnson, E. Palecek, *Anal. Chem.* 67 (1996) 4065.
- [6] E. Palecek, M. Fojta, *Anal. Chem.* 73 (2001) 75A.
- [7] R. Hirsch, E. Katz, I. Willner, *J. Am. Chem. Soc.* 122 (2000) 12053.
- [8] L.S. Ichia, E. Katz, J. Wasserman, I. Willner, *Chem. Commun.* (2002) 158.
- [9] J. Wang, A. Kawde, A. Erdem, M. Salazar, *Analyst* 126 (2001) 2020.
- [10] E. Palecek, S. Biilova, L. Havran, R. Kizek, A. Miculkova, F. Jelen, *Talanta*, in press.
- [11] MCB1200 MixSep Technology, [http://www.sigris.com/mcb\\_technology.html](http://www.sigris.com/mcb_technology.html).



## Genomagnetic electrochemical assays of DNA hybridization

Joseph Wang \*, Danke Xu, Arzum Erdem <sup>1</sup>, Ronen Polsky, Marcos A. Salazar

*Department of Chemistry and Biochemistry, College of Arts and Sciences, New Mexico State University, Las Cruces, NM 88003-8001, USA*

Received 10 May 2001; received in revised form 2 August 2001; accepted 2 August 2001

### Abstract

An electrochemical genomagnetic hybridization assay has been developed to take advantage of a new and efficient magnetic separation/mixing process, the amplification feature of enzyme labels, and single-use thick-film carbon transducers operated in the pulse-voltammetric mode. It represents the first example of coupling a magnetic isolation with electrochemical detection of DNA hybridization. The new protocol employs an enzyme-linked sandwich solution hybridization, with a magnetic-particle labeled probe hybridizing to a biotinylated DNA target that captures a streptavidin-alkaline phosphatase (AP). The  $\alpha$ -naphthol product of the enzymatic reaction is quantitated through its well-defined, low-potential (+0.1 V vs. Ag/AgCl) differential pulse-voltammetric peak at the disposable screen-printed electrode. The efficient magnetic isolation is particularly attractive for electrical detection of DNA hybridization which is commonly affected by the presence of non-hybridized nucleic acid adsorbates. The new biomagnetic processing combines such magnetic separation with a low-volume magnetic mixing, and allows simultaneous handling of 12 samples. The attractive bioanalytical behavior of the new enzyme-linked genomagnetic electrical assay is illustrated for the detection of DNA segments related to the breast-cancer *BRCA1* gene. © 2002 Elsevier Science B.V. All rights reserved.

**Keywords:** DNA assay; Electrochemistry; Magnetic separation; Enzyme label

### 1. Introduction

Electrochemical devices have received considerable attention in the development of DNA hybridization biosensors [1–3]. The high sensitivity of electrochemical transducers, coupled with their compatibility with modern microfabrication and

miniaturization technologies, low cost and power requirements, and independent of sample turbidity, make such devices excellent candidates for DNA diagnostics.

Electrochemical DNA biosensors commonly rely on the conversion of the hybridization event into useful electrical signals. The base-pairing recognition event can be detected via the increased current signal of a redox indicator [4,5], from changes in the intrinsic electroactivity of the nucleic acid [6,7], from changes in interfacial parameters such as capacitance or conductivity [8,9], or in connection to the use of enzyme labels

\* Corresponding author. Fax: +1-505-646-2649.  
E-mail address: joewang@nmsu.edu (J. Wang).

<sup>1</sup> On leave from Ege University, Faculty of Pharmacy, 35100 Bornova-Izmir, Turkey.

[10,11]. Such labels have been widely used in electrochemical immunoassays [12,13], and hold great potential for electrical detection of DNA hybridization. Such promise is attributed to the biocatalytic activity of these labels that provides the amplification essential for monitoring very low target levels. This can be accomplished by combining the hybridization step with an electrochemical measurement of the product of the enzymatic reaction. The great potential of enzyme labels for electrical detection of DNA hybridization was demonstrated first using horseradish peroxidase [10], and more recently in connection to alkaline phosphatase (AP) [11].

This article describes an effective and simple genomagnetic electrochemical assay based on the coupling of a new biomagnetic processing technique with the use of AP enzyme label and single-use microfabricated thick-film electrochemical transducers (Fig. 1). Magnetic fields have recently found considerable application throughout life sciences. The use of magnetic particles can bring novel capabilities to bioaffinity assays and sensors. Bioanalysis has benefited from the use of magnetic beads in electrochemical immunosensors [14,15] or for fluorescence DNA hybridization assays [16], but not in connection to electrical detection of DNA hybridization. The new biomagnetic processing technology, employed in the

present study, combines efficient magnetic mixing and separation into a single mechanism [17]. Such MixSep™ Technology process thus integrates, on the same platform, the isolation of the target nucleic acid with an efficient low-volume magnetic mixing during the hybridization, enzyme association, and substrate–enzyme reaction steps (Fig. 1b–d, respectively). Up to 12 assays can be performed simultaneously using the same compact commercial (MCB 1200) unit. The efficient magnetic ‘removal’ of non-hybridized DNA is particularly attractive for electrical biosensing of DNA hybridization that is often hampered by errors due to non-specifically adsorbed oligonucleotides. The minimization of contributions from these non-hybridized nucleic acids is the main focus of this article. The successful coupling of the biomagnetic separation/mixing platform with the advantages and improvements of AP enzyme labels and pulse-voltammetric detection of the enzymatically-liberated naphthol product at disposable screen-printed strip electrodes (step e, Fig. 1) is reported in the following sections. Such single-use thick-film transducers are particularly attractive for decentralized DNA testing.

## 2. Experimental

### 2.1. Apparatus

A CH instruments Electrochemical analyzer (CHI, Austin, TX) was used for the pulse-voltammetric measurements in connection with a Packard Bell multimedia C75 personal computer and the CHI 620 software. The microsphere preparation, the hybridization event, the enzyme binding, and the biocatalytic reactions were performed with the MCB 1200 Biomagnetic Processing Platform (Dexter Magnetic Technologies, Fremont, CA).

### 2.2. Electrode preparation

The screen-printed electrodes (SPEs) were fabricated using a semi-automatic screen printer (Model TF-100, MPM Inc., Franklin, MA). The carbon ink (Acheson 440B, Acheson Colloid Co.,

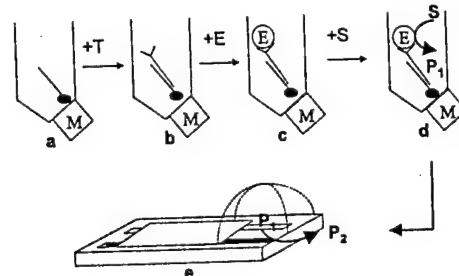


Fig. 1. Schematic representation of the analytical protocol: (a) introduction of the oligomer-coated beads; (b) addition of the biotinylated target (T) oligomer-hybridization event; (c) addition of the streptavidin-enzyme (E = alkaline phosphatase) and its conjugation with the biotinylated target (of the duplex); (d) addition and enzymatic reaction of the substrate (S =  $\alpha$ -naphthyl phosphate); (e) placement of a droplet of the supernatant onto the thick-film electrode for the voltammetric measurement.

Ontario, CA) was printed onto alumina ceramic plates ( $33.5 \times 101.5$  mm $^2$ , Coors Ceramic Co., Golden, CO) through a patterned stencil to give a group of 10 working electrodes. The printed electrodes were subsequently cured for 60 min at 150 °C, and then allowed to cool. A parallel Ag/AgCl layer was printed using a Ag/AgCl ink (Erccon R414, Wareham, MA). An insulator layer (based on a ESL protective ink 240-5B; ESL Inc., King of Prussia, PA) was subsequently printed for exposing  $2.0 \times 6.0$  mm $^2$  working electrode area. All SPEs were pretreated by scanning the potential between –0.5 and +1.0 V at 100 mV s $^{-1}$  for 10 cycles in a phosphate buffer (0.2 M, pH 7.4) solution.

### 2.3. Materials and reagents

All stock solutions were prepared using deionized and autoclaved water. Sodium dodecyl sulfate (SDS), NaHCO<sub>3</sub> and Na<sub>2</sub>CO<sub>3</sub> were purchased from JT Baker. Tween 20, MgSO<sub>4</sub> and NaClO<sub>4</sub> were purchased from Aldrich. Tris-HCl buffer, LiCl, Na<sub>2</sub>EDTA, NaOH, NaCl, streptavidin-AP,  $\alpha$ -naphthol and  $\alpha$ -naphthyl phosphate were purchased from Sigma. Proactive streptavidin-coated micro spheres (0.8  $\mu$ m diameter, CMO1N-lot 4725) were purchased from Bangs Laboratories (Fishers, IN). Oligonucleotides (with 5' biotin modification) were acquired from Sigma-Genosys Ltd. and had the following sequences:

Immobilized probe: E908X-WT(P): biotin-5'GAT TTT CTT CCT TTT GTT C  
 Target: E908X-WT: biotin-5'GAA CAA AAG GAA GAA AAT C  
 Non-complementary oligomer: biotin-5'GGT CAG GTG GGG GGT ACG CCA GG.

### 2.4. Preparation of oligomer-coated microspheres and analytical procedure

The bead preparation (performed on the MCB 1200 Biomagnetic Processing Platform) was carried out using a modified procedure recommended by Bangs Laboratories [18]. Briefly, 1.0 mg of streptavidin-coated magnetic beads was transferred into a 1.5 ml centrifuge tube. The microspheres were washed with 200  $\mu$ l TTL buffer (100

mM Tris-HCl, pH 8.0, and 0.1% Tween 20, 1 M LiCl) and resuspended in 20  $\mu$ l TTL buffer. Twenty-five micrograms probe oligomer was added and incubated for 15 min at room temperature with gentle mixing. The immobilized probe was then separated, and washed with 100  $\mu$ l 0.15 NaOH, followed by 200  $\mu$ l TT buffer (250 mM Tris-HCl, pH 8.0, and 0.1% Tween 20), and 200  $\mu$ l TTE buffer (250 mM Tris-HCl, pH 8.0, 0.1% Tween 20/20 mM Na<sub>2</sub>EDTA, pH 8.0). The preparation process was completed by resuspending the coated beads in a 100  $\mu$ l TTN buffer (0.5 M NaClO<sub>4</sub>, 20 mM MgSO<sub>4</sub>, 0.1% SDS) for storage at +4 °C until use.

Prior to the hybridization, 5  $\mu$ l of the resulting solution (containing 50  $\mu$ g probe-coated spheres) was added into a 1.5 ml centrifuge vial, washed twice with TT buffer, separated and spiked with hybridization solution (750 mmol l $^{-1}$  NaCl and 75 mmol l $^{-1}$  sodium citrate) up to a total volume of 50  $\mu$ l (Fig. 1a). The desired amount of the target was then added, and the hybridization reaction was carried out (usually for 20 min) under magnetic stirring at room temperature (Fig. 1b). The hybridized microsphere conjugates were then washed twice with TT buffer and resuspended in 50  $\mu$ l TTL buffer, containing 1 unit streptavidin-AP, with magnetic mixing for 25 min (Fig. 1c). The enzyme labeled conjugates were then washed twice with TT buffer, resuspended in 100  $\mu$ l of a 20 mM  $\alpha$ -naphthyl phosphate solution (prepared in 0.5 M NaHCO<sub>3</sub>/Na<sub>2</sub>CO<sub>3</sub> buffer, pH 9.5) and incubated for 20 min at room temperature (Fig. 1d). A 100  $\mu$ l droplet of the supernatant was then placed onto the working area of the SPE (Fig. 1e). The  $\alpha$ -naphthol product of the enzymatic reaction was measured using a differential pulse-voltammetric scan from –0.20 to +0.40 V, with a rate of 20 mV s $^{-1}$  and an amplitude of 50 mV.

### 3. Results and discussion

The new electrochemical DNA hybridization sensor system couples an efficient magnetic isolation with a sandwich solution hybridization, enzyme amplification, and differential pulse-voltammetric detection at SPEs (Fig. 1). It

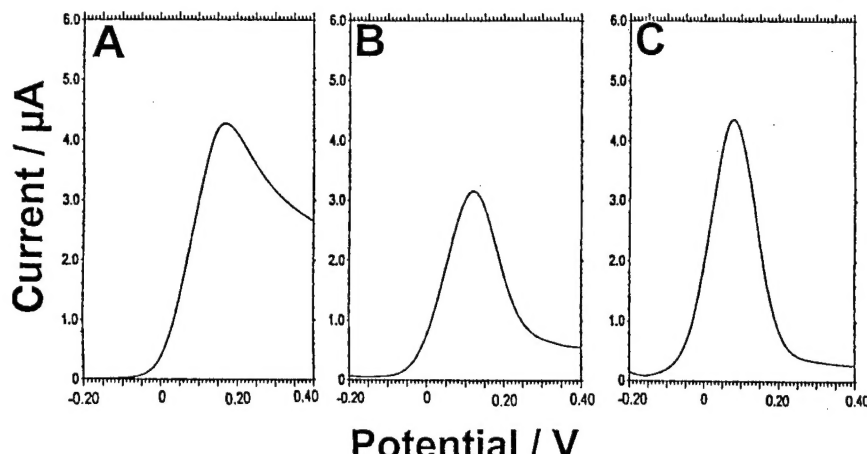


Fig. 2. Effect of the voltammetric waveform upon the response of  $2 \times 10^{-4}$  M  $\alpha$ -naphthol. (A) Linear sweep voltammetry; (B) square wave voltammetry; and (C) differential pulse voltammetry; scan rate (A–C) and amplitude (B, C), 20 mV s<sup>-1</sup> and 50 mV, respectively. Electrolyte, 0.5 M NaHCO<sub>3</sub>/Na<sub>2</sub>CO<sub>3</sub> buffer (pH 9.5).

represents the first coupling of magnetic separation and electrical detection of DNA hybridization. A new biomagnetic processing technology, combining an efficient and simultaneous low-volume magnetic isolation and mixing [17], has been employed. The characterization and optimization of the resulting genomagnetic enzyme-linked electrical protocol are illustrated below for assays of short DNA fragments related to the *BRCA1* breast-cancer gene [19]. As needed for meeting the demands of decentralized genetic testing, the new assay employs microfabricated and disposable thick-film electrode transducers.

AP is a suitable enzyme for electrochemical assays since it catalyzes the conversion of electroinactive phenyl phosphate substrates to electroactive phenolic products. The use of the  $\alpha$ -naphthyl phosphate substrate is particularly attractive due to the low-potential of the liberated  $\alpha$ -naphthol. Fig. 2 compares different voltammetric methods for detecting  $\alpha$ -naphthol at the thick-film carbon transducer. The three techniques yield a well-defined oxidation peak with a peak potential of around +0.10 V. Most favorable signal-to-background characteristics and peak shape are observed using the differential pulse waveform (C). This mode was employed throughout this study. The favorable response of Fig. 2 indicates also that the use of screen-printed transducers

does not compromise the voltammetric behavior. Such disposable electrode strips also address the electrode fouling problem (associated with the oxidation of phenolic compounds) and are advantageous for decentralized DNA testing.

The efficient magnetic isolation of the probe-target DNA duplex is particularly attractive for electrochemical DNA biosensors that are often prone to errors associated with non-specific adsorption effects. Careful control of the surface architecture (mixed oligonucleotide/‘blocking’ layer) is commonly used to minimize the effect of non-complementary DNA adsorbates [1–4, 20]. The magnetic separation and removal of non-hybridized oligomers obviate the need for such deliberate time-consuming surface modification and enables selective electrical detection of the target nucleic acid. Such improvements are illustrated in Fig. 3 in connection to the measurements of the breast-cancer target oligonucleotide in the presence of a large (five-fold) excess of a non-complementary oligomer. Unlike the large, well-defined response observed for 3 ppm of the target (A,a), 15 ppm of the non-complementary strand displays a very small signal (A,b), which is slightly larger than the corresponding ‘blank’ voltammogram (A,c). Note that such a favorable behavior is observed at the bare electrode strip (without any ‘blocking’ layer). The mixture analysis (of Fig.

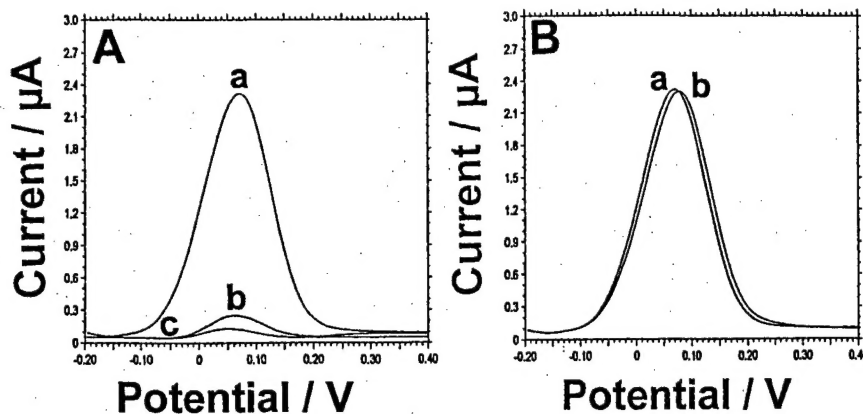


Fig. 3. Differential pulse voltammograms for: (A) 3 ppm ( $\text{mg l}^{-1}$ ) target (a); 15 ppm non-complementary oligomer (b); and blank/control (c). Voltammograms for: (B) 3 ppm target (a); a mixture of the target (3 ppm) and a non-complementary oligomer (15 ppm) (b). Hybridization solution (750  $\text{mmol l}^{-1}$  NaCl and 75  $\text{mmol l}^{-1}$  sodium citrate); hybridization time, 10 min; enzyme association time, 25 min; substrate concentration, 20 mM; enzymatic reaction time, 20 min; voltammetric scan and electrolyte, as in Fig. 2C.

3B) further demonstrates the efficient removal of non-complementary nucleic-acid adsorbates and the resulting minimization of non-specific binding effects. The large excess of the non-complementary oligomer has a negligible effect upon the current response of the target (compare a and b). Other potential interferences, e.g. coexisting redox-active constituents, are also expected to be eliminated by the magnetic isolation.

Various parameters involved in the new geno-magnetic protocol were examined and optimized. Fig. 4 shows the influence of the amount of the magnetic beads upon the voltammetric response. The response increases nearly linearly up to 50  $\mu\text{g}$ , then more slowly, and levels off above 75  $\mu\text{g}$ . Subsequent work thus employed 50  $\mu\text{g}$  particles. Based on the binding capacity of the spheres (19  $\mu\text{g}$  biotinylated probe per 1 mg) [18], such amount corresponds to 950 ng probe. (A larger amount, of 25  $\mu\text{g}$  biotinylated probe per 1 mg spheres, was employed during the coating step to assure a full surface coverage.)

Each step of the assay was optimized. Fig. 5 displays the optimization of the duration of the various steps of the assay. The voltammetric peak current increases nearly linearly with the hybridization time between 2 and 20 min and then it levels off (A). The binding time of the streptavidin-AP with the biotinylated target (after

the hybridization) also has a profound effect upon the response (B). The current increases slowly with the enzyme conjugation period at first (up to 10 min), then more rapidly, and levels off above 25 min. Another parameter that affects the observed peak is the amount of time in which the enzymatic reaction is allowed to proceed. Fig. 5C examines the effect of the length of the enzymatic reaction (after addition of the naphthyl-phosphate substrate). The voltammetric response rises nearly linearly with the reaction time up to 10 min, then more slowly, and levels off after about 20 min. All subsequent work employed 25 and 20 min enzyme association and reaction times, respectively. Such periods correspond to assay cy-

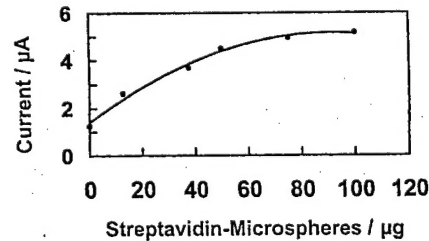


Fig. 4. Effect of the amount of oligomer-coated microspheres upon the voltammetric response of the DNA assay. Target concentration, 10 ppm; hybridization time, 50 min. Other conditions, as in Fig. 3.

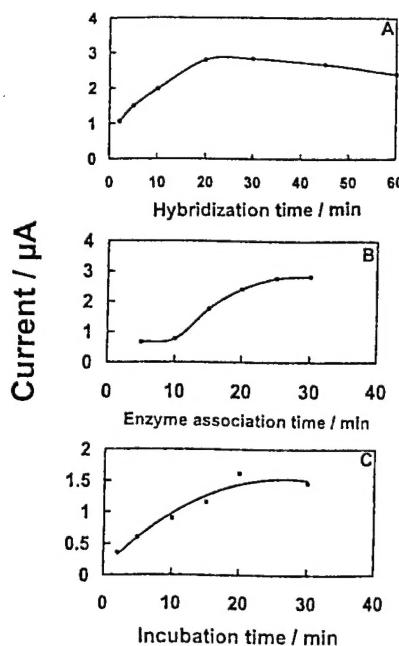


Fig. 5. (A) Effect of the hybridization time. (B) Effect of the association time between the biotinylated oligomer and streptavidin-alkaline phosphatase. (C) Effect of the  $\alpha$ -naphthyl phosphate reaction time. Target concentration, 10 ppm. Other conditions, as in Fig. 4.

cles of about an hour in connection to 10–20 min hybridization times. It should be pointed out that the new MCB 1200 Biomagnetic processing system can handle up to 12 samples simultaneously to significantly reduce the actual assay time [17].

Good precision is another attractive feature of the present enzyme-linked genomagnetic electrical assay. The new magnetic processing is based on a rotating magnetic field that mixes the paramagnetic particles in a highly reproducible fashion (without shaking or stirring the test medium). A series of six repetitive hybridization measurements of 10 ppm of the breast-cancer DNA target thus resulted in a reproducible voltammetric signal, with a mean peak current of 4.7  $\mu$ A and a relative standard deviation of 7.0% (conditions, as in Fig. 4; not shown). Such precision reflects also the reproducibility of the screen-printing fabrication.

As expected for bioaffinity assays, the linear range and overall sensitivity are strongly influenced by the hybridization time. Fig. 6 displays voltammograms for two calibration experiments

involving increasing target concentration over the 0.25–1.0 ppm (A) and 1–8 ppm (B) ranges in connection to 20 and 5 min hybridization, respectively. In both experiments, the peak current increases linearly with the target concentration to yield highly linear calibration plots (shown as insets). Such plots are characterized by a sensitivity of 2.240 (A) and 0.258 (B)  $\mu$ A ppm<sup>-1</sup>, and correlation coefficients of 0.996 and 0.995, respectively. A substantial curvature was observed for

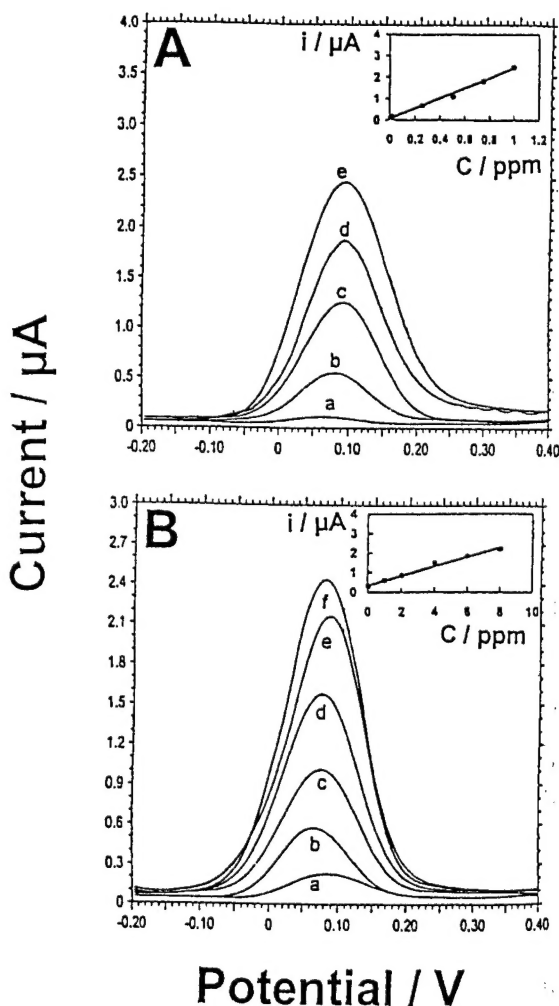


Fig. 6. Differential pulse voltammograms for different target concentrations: (A) (a) 0, (b) 0.25, (c) 0.5, (d) 0.75, and (e) 1.0 ppm; (B) (a) 0, (b) 1.0, (c) 2.0, (d) 4.0, (e) 6.0, and (f) 8.0 ppm; hybridization time, 20 (A) and 5 (B) min; other conditions, as in Fig. 4. Also shown (insets), the resulting calibration plots.

target concentrations higher than 1.5 ppm in connection to 20 min hybridization (not shown). Such curvature is attributed to surface saturation (associated with the hybridization capacity of the coated spheres).

The data of Fig. 6A(b) indicate that the coupling of efficient magnetic mixing, enzyme amplification, and pulse-voltammetric detection allows the detection of low target concentrations. The detection limit was estimated from measurements of 100 ppb of the breast-cancer oligonucleotide in connection to a 20 min hybridization period (not shown). A value of 10 ppb could thus be estimated based on the signal-to-background characteristics of these data. Such detection limit corresponds to 500 pg target in the 50  $\mu$ l sample volume. Substantially lower detection limits are expected in connection to surface accumulation of the product of the enzymatic reaction [15], to longer hybridization times, or via minimization of AP adsorption onto the walls of the centrifugal vial (that appears to be responsible for the 'blank' peak (of Fig. 6A(a)), or by combining these avenues.

In conclusion, we demonstrated for the first time the coupling of magnetic separation and electrochemical detection of DNA hybridization. The new enzyme-linked genomagnetic electrical assay yields a very attractive bioanalytical performance. The efficient magnetic isolation is particularly attractive for electrical detection of DNA hybridization which is often influenced by the presence of non-hybridized nucleic acids. Other electrochemical schemes for detecting DNA hybridization should greatly benefit from such minimization of non-specific adsorption processes. Preliminary work on the coupling of adsorptive stripping hybridization detection with the magnetic isolation of the duplex is very encouraging, including an effective discrimination against a large excess of coexisting mismatched and non-complementary oligomers, chromosomal DNA, RNA and proteins, and the use of longer DNA targets. The immobilization of the probe onto the magnetic beads rather than onto an electrode offers also greater versatility. Current work in our laboratory aims at developing microfluidic devices, integrating and automating the various

steps of the present protocol and performing multiple such parallel assays on a single microfluidic chip platform. We are developing new powerful protocols coupling the magnetic separation/mixing with nanoparticle metal tags and highly-sensitive stripping-voltammetric detection of the dissolved tag. These, and similar applications of magnetic particles in nucleic-acid assays can bring novel capabilities to the area of genetic testing.

### Acknowledgements

Financial support from the US Army Medical Research (Award No. DAMD17-00-1-0366) and the National Institutes of Health (Grant No. R01 14549-02). A.E. acknowledges the NATO fellowship from The Turkish Scientific Research and Technical Council (TUBITAK). M.A.S. acknowledges support from the RISE program at NMSU. A loan of the MCB1200 Biomagnetic Processing Platform, provided by S. Crouch (Dexter Magnetic Technologies Inc.), is gratefully acknowledged.

### References

- [1] E. Palecek, M. Fojta, *Anal. Chem.* 73 (2001) 75A.
- [2] S.R. Mikklesen, *Electroanalysis* 8 (1996) 15.
- [3] J. Wang, *Chem. Eur. J.* 5 (1999) 1681.
- [4] S. Takenaka, K. Yamashita, M. Takagi, Y. Uto, H. Kondo, *Anal. Chem.* 72 (2000) 1334.
- [5] J. Wang, X. Cai, G. Rivas, H. Shiraishi, *Anal. Chim. Acta* 326 (1996) 141.
- [6] D.H. Johnston, K. Glasgow, H.H. Thorp, *J. Am. Chem. Soc.* 117 (1995) 8933.
- [7] J. Wang, G. Rivas, J. Fernandes, J.L. Paz, M. Jiang, R. Waymire, *Anal. Chim. Acta* 375 (1998) 197.
- [8] C. Berggren, P. Stalhandske, J. Brundell, G. Johansson, *Electroanalysis* 11 (1999) 156.
- [9] J. Wang, M. Jiang, A. Fortes, B. Mukherjee, *Anal. Chim. Acta* 402 (1999) 7.
- [10] T. de Lumley, C. Campbell, A. Heller, *J. Am. Chem. Soc.* 118 (1996) 5504.
- [11] O. Bagel, C. Degrand, B. Limoges, M. Joannes, F. Azek, P. Brossier, *Electroanalysis* 12 (2000) 1447.
- [12] W.R. Heineman, H.B. Halsall, *Anal. Chem.* 57 (1985) 1321.
- [13] P. Skladal, *Electroanalysis* 9 (1997) 737.
- [14] A.G. Gehring, J.D. Brewster, P.L. Irwin, S.I. Tu, L.J. Van Houten, *J. Electroanal. Chem.* 469 (1999) 27.